CHITOSAN COMPOSITE CRYOGEL WITH POLYELECTROLYTE COMPLEXES FOR TISSUE REGENERATION APPLICATION

Bolat Sultankulov

A thesis submitted in partial fulfillment of the requirement of Nazarbayev University for the degree of Doctor of Philosophy in Science, Engineering and Technology

2020

ABSTRACT

Chitosan has been a successful choice for tissue-engineering applications over the last few decades. Chitosan is a natural polysaccharide with excellent properties for tissue engineering applications, such as biodegradability, biocompatibility, and antimicrobial activity. Available free amine groups in its structure allows further chemical modifications, so new properties could be added for specific tissue engineering application. This dissertation highlights the advances made in biomaterial production and describes novel polyelectrolyte-based (PEC) cryogel that contains chitosan (CHI) and heparin (Hep). We will discuss the preparation of new cryogel material and its physico-chemical properties. Additionally, the measurement of biological activity would be addressed *in vitro* and *in vivo*. In particular, the cryogels obtained will be tested to induce differentiation of mesenchymal stem cells (rat BMSCs) derived from rat bone marrow into the osteogenic lineage. Additionally, this study will show potential uses of novel PEC-based cryogel for skin regeneration *in vitro* and *in vivo*, demonstrating the broad application of established scaffolding.

The research in this dissertation is important because it demonstrates the efficacy of PEC cryogels for tissue engineering applications. This is the first PEC cryogel scaffold based on CHI-Hep made from a one-step reaction with effective loading of growth factors and cytokines.

TABLE OF CONTENTS

LIST OF TABLES

LIST OF FIGURES

Figure 10. Biological activity experiments. (a) Inhibition of NMuMG proliferation by the cryogel released TGF-β, (b) Stimulation of MC/9 proliferation by the cryogel released IL-10, (c) Stimulation of HUVEC proliferation by the cryogel released VEGF, (d) Decrease in the wound area by the cryogel released FGF, (e) Wound areas are quantified in panel d. Data were analyzed using one-way ANOVA with Bonferroni's multiple comparisons test. $^{**}p < 0.01$, $^{***}p < 0.001$, $^{****}p < 0.0001$ compared with the control group.

Figure 11. Wound healing after treatment with different cryogel groups: treated with cryogel alone, cryogel + IL-10/TGF-β, cryogel +VEGF/FGF and cryogel + all factors (GF/C). Wound area changes over time are shown (% vs. Day 0). Wound areas in the fourth group (cryogel + GF/C) significantly decreased on days 7 and 10 in comparison to the other groups. Values: mean ± SE. $^{***}p < 0.01$ compared to other groups, $^{*}p < 0.05$ compared to cryogel alone group.

Figure 12. Wound healing and epithelial regeneration. (a) Sample images of wound closure on day 10. (b) Wound area (% vs. Day 0) over time. Wound areas in the cryogel+GF/C group significantly decreased on days 7 and 10 in comparison to others. (c) Wound epithelization. Epithelialization was evaluated as CEL and REL. Total epithelial length (CEL+REL) increased with time in all groups, with the same CEL among all groups. REL in cryogel+GF/C on day 10 was significantly longer in comparison to other groups. n=5. Bar=100 μm. Values: mean ± SE. $^{*}p < 0.05$ compared to the no treatment group and group with cryogel alone, $^{\#}p < 0.05$ compared to the no treatment group.

Figure 13. Development of granulation tissue and collagenosis. (a)Representative images of MT stained (blue) granulation tissues in each group (parenthesized in red). (b) Data of measured thickness and collagenosis in the tissues. The data collected by a morphometrical method. Granulations in the groups with cryogel alone and

cryogel+GF/C were significantly thicker in comparison to no treatment group. Collagenosis in the group with cryogel+GF/C progressed significantly as compared to the group with no treatment group. n=5. Bar=100 μm. Values: mean ± SE. *$p < 0.05$, **$p < 0.01$ compared to the no treatment group.

LIST OF SYMBOLS

$m_{swollen}$	Mass of swollen cryogel
m_{dry}	Mass of dry cryogel
$m_{squezzed}$	Mass of squeezed cryogel
$\alpha(\%)$	The degree of degradation
m_i	Mass initial
m_f	Mass final
η (Pas)	Viscosity, Pascal
$\dot{y}$	Shear rate

LIST OF ABBREVIATIONS

BMP-2	Bone morphogenetic protein 2
CHI	Chitosan
DD	Degree of deacetylation
ECM	Extracellular matrix
FGF	Fibroblast growth factor
GA	Glutaraldehyde
GF/C	Growth factors/cytokine
HA	Hydroxyapatite
IL-10	Interleukin 10
IPC	non-stoichiometric interpolymer complex
MSC	Mesenchymal stem cells
PEC	Polyelectrolyte complex
PVA	Polyvinyl alcohol
Rat BMSCs	Rat bone marrow-derived mesenchymal stem cells
TGF-β	Transforming growth factor-beta

VEGF	Vascular endothelial growth factor

DECLARATION

I declare that the research contained in this thesis, unless otherwise formally indicated within the text, is the original work of the author. The thesis has not been previously submitted to this or any other university for a degree and does not incorporate any material already submitted for a degree.

Signed

Dated

ACKNOWLEDGMENTS

I would like to thank my supervisors. Dr Tursonjan Tokay, Dr Arman Saparov, Dr Dmitriy Berillo, and Dr Lyuba Mikhalovka for supporting my research project and for their patience. I would like to thank Dr Sergey Mikhalovsky for giving me an opportunity to visit the University of Brighton and conduct important experiments. In terms of research, the support of Dr Arman Saparov was central to all the work presented in this thesis. Also, I would like to thank Dr Luis R. Rojas-Solórzano, for his dedication to his work and support to all PhD students at Nazarbayev University.

Finally, I am grateful to my family, my mother for always believing in me, my wife for always supporting me throughout this academic journey, and to my newborn son Arlan for his smiles and emotions.

CHAPTER 1. INTRODUCTION

The main objective of the current work is the design of biocompatible biomaterials based on CHI and synthetic polymers, capable of binding active biological molecules such as various growth factors and cytokines. An obtained scaffold should be able to promote regeneration of the bone and skin either by stimulation of cell proliferation or by differentiation of stem cells. During the design, it is important to understand the properties of its main component CHI, and how it is used in tissue engineering. This chapter summarizes the progress made in developing CHI-based biomaterials for tissue engineering applications, in particular for bone and skin regeneration. More details on the main objectives of the present thesis are represented and the part of the work in this Chapter has been published in [1,2].

1.1 Chitosan-natural polymer for tissue engineering

Biomaterial design is an active research field to develop scaffolds for the regeneration of disease- or injury-damaged tissues and organs. A crucial step in tissue engineering and regenerative medicine is the identification and design of suitable materials for tissue engineering [3]. Owing to their biocompatibility and structural similarity with the extracellular matrix components, greater attention has been dedicated to natural polymers over the past decades. The wide availability and specific biological activity of each natural polymer make them a suitable candidate for the production of new natural or/and semi-synthetic materials closely resembling the natural structure and tissue functionality necessary for successful regeneration. Starch, collagen, alginate, cellulose, hyaluronic acid, chitin, and CHI are attractive natural polymers for scaffold design which could be used for the regeneration of the tissues. CHI is a chitin-derived linear natural carbohydrate biopolymer with structural similarities to extracellular matrix (ECM) glycosaminoglycans (GAGs) involved in cell-cell adhesion [4]. The

hydrophilic structure of CHI facilitates the cell adhesion, proliferation, and differentiation of different cell types and the polycationic structure of mildly acidic CHI allows the immobilization of negatively charged enzymes, proteins, and DNA [5,6]. CHI could be designed for tissue engineering and regenerative medicine in various forms, such as hydrogels, sponges, fibers, sheets, films, and other structures [7]. One critical direction in the development of biomaterials is the possibility to load specific active molecules, such as growth factors and cytokines [8]. CHI's polycationic nature enables the direct loading of various proteins and molecules and the introduction of specific complexes, such as a polyelectrolyte complex (PEC) [9]. PECs are formed by electrostatic interaction between oppositely charged molecules. PECs avoid the use of chemical cross-linking agents and thus the potential for toxicity and other undesired effects [10]. PEC forms between CHI and heparin (Hep) in the form of a hydrogel and this configuration allows loading of different bioactive molecules which could be used to different tissue regeneration applications [11].

1.2 Structure and properties of chitosan

Chitin is the second most abundant natural polymer [12] and consists of 2-acetamido-2-deoxy-β-D-glucose via a β (1 –4) link and is usually derived from marine crustaceans, insects or fungi. Due to its insolubility in water and most organic solvents, its use in scaffold fabrication is limited. CHI is a linear polysaccharide derived from partial chitin deacetylation as shown in Figure 1.

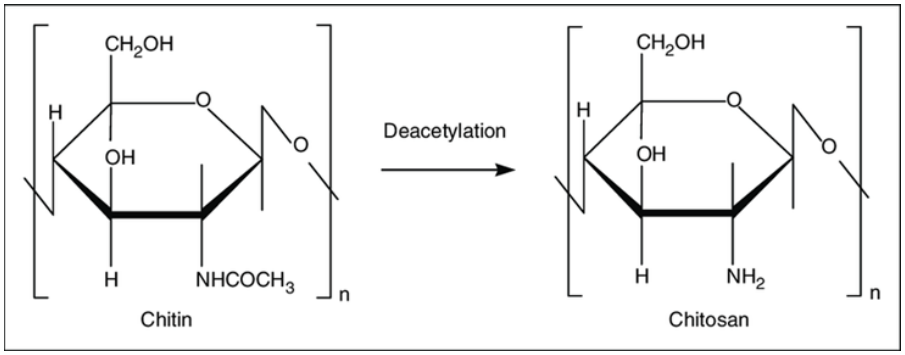

Figure 1. Chitin deacetylation to chitosan.

It is a copolymer of randomly located (1–4)-2-acetamido-2-deoxy-β-D-glucan (N-acetyl D-glucosamine) and (1–4)-2-amino-2-deoxy-β-D-glucan (D-glucosamine) units. The number of amino groups as a ratio between of D-glucosamine to the sum of D-glucosamine and N-acetyl D-glucosamine known as a deacetylation degree (DD) and should be not less than 60% for CHI. Chitin deacetylation is performed by chemical hydrolysis (alkaline conditions) [13] or by enzymatic hydrolysis (chitin deacetylase) [14]. CHI is soluble in dilute organic acids such as acetic acid [15], as well as diluted hydrochloric acid, alteration of CHI structure is possible due to the presence of amino groups [12]. CHI fungal sources are more favored on an industrial scale due to narrower molecular mass distribution, year-round availability, more regulated and scalable production, and less immunogenicity compared to seafood sources, which could cause allergies and restrict biomedical applications [13]. Chitin from seafood and fungi is covalently linked to glucans and glycosylated proteins which are the cause of the strong immunological response. However, after purification, fungal chitin particles are more homogeneous and smaller in size, which results in less immunogenicity due to the less aggressive phagocytosis [16].

The physical properties of CHI depend on several factors, such as molecular weight, DD, and product purity [17]. CHI solubility is pH-dependent [18] and soluble in dilute acids produced by the protonation of the amino groups of D-glucosamine residues [19]. Available amino groups allow CHI to form complexes with metal ions [20,21], natural or synthetic anionic (poly(acrylic acid)) polymers [22], lipids, proteins, and DNA. CHI based scaffolds are usually cross-linked by glutaraldehyde, oxidized dextran, or other oxidized carbohydrates, 1,1,3,3-tetramethoxypropan, and genipin [22–24]. It is important to mention that CHI is a unique positively charged semi-natural polysaccharide [25] and the property is used to produce CHI based PEC films via layer-by-layer deposition technique [22]. Its amino groups could react with aldehyde groups by reductive amination [15] and hydroxyl groups enable its

etherification and esterification [26]. Furthermore, CHI has such essential properties as high biocompatibility, biodegradability, antibacterial activity, non-antigenicity, and high adsorption properties that make it a strong candidate for tissue engineering and other biomedical applications [14].

1.3 Objectives and structure of the thesis

The main aim of the thesis was to develop and evaluate the efficacy of PEC-based biomaterial for tissue regeneration applications. The objectives required to achieve the main objectives were:

Choose the right polymers for cryogel synthesis with the ability to form PEC;

Evaluate the physico-chemical properties of obtained cryogels by conducting mechanical testing, FTIR, assess swelling and porosity, conduct *in vitro* degradation experiments and describe rheological properties;

Assess the efficacy of obtained cryogels in loading growth factors and defining the release kinetics profile;

Evaluate the biological activity of cryogel loaded with growth factors and cytokines for wound healing and osteogenic differentiation of rat bone marrow-derived mesenchymal stem cells (rat BMSCs);

Assess the efficacy of cryogel *in vivo* in wound healing application.

Six chapters are included in the PhD thesis. The first chapter describes the role of CHI in tissue engineering applications.

Chapter 2 details the use of CHI in wound healing and bone regeneration applications, including the different types of scaffolding and their biological activity.

Chapter 3 describes the synthesis and characterization of obtained cryogel and its application for the differentiation of rat BMSCs into osteogenic lineage *in vitro*.

Chapter 4 presents *in vitro* and in *vivo* data on the use of obtained cryogels for wound healing applications in collaboration with Dr Shiro Jimi from Fukuoka University

(Japan). All the *in vivo* experiments were conducted by Dr Jimi, in vitro experiments were conducted by me, Alexandr Jakuparov and Ayan Nurkesh.

1.4 Role of Collaborators

The current dissertation is a multidisciplinary study aimed at developing a novel PEC-based CHI scaffold for tissue engineering applications. This thesis was supported by the Ministry of Education and Science of the Republic of Kazakhstan, which financed the PhD program at the University of Nazarbayev, and was also supported by the Erasmus+ Key Action 1 program of the European Union, which financed three-month mobility training at the University of Brighton (UK).

All aspects of this thesis have been reviewed by the team of supervisors: Dr Tursonjan Tokay, Dr Arman Saparov, Dr Dmitriy Berillo, and Dr Lyuba Mikhalovska. Productive suggestions were made by Dr Dmitry Berillo, Dr Lyuba Mikhalovska, and Professor Sergey Mikhalovsky during and after three months of training at the University of Brighton. Other collaborations include Dr Shiro Jimi from Fukuoka University (Japan), this collaboration was established by Dr Arman Saparov and this collaboration resulted in the evaluation of obtained cryogel for wound healing application in mice and presentation of the results at international conferences and publication [27]. Suggestions and feedback on manuscripts were provided by my supervisors: Dr Tursonjan Tokay, Dr Arman Saparov, Dr Dmitriy Berillo, and Dr Lyuba Mikhalovska. Several contributions were also received from the colleagues working at the National Laboratory of Astana of Nazarbayev University including Dr Sholpan Askarova, Sholpan Kauanova, Yulya Yantcen, Dr Andrei Coi, Baurzhan Negmetzhanov, Dr Aidos Baumuratov, and Nurlan Mansurov. The contribution was also done by colleagues and medical students from Nazarbayev University School of Medicine including Ayan Nurkesh, Alexandr Jaguparov, and Saltanat Smagul.

This thesis is based on my work, and it was written by me. Individual contributions are described in detail in the contribution section of the author, where applicable.

1.5 Thesis outputs

Journal articles

[1] Sultankulov, B., Berillo, D., Sultankulova, K., Tokay, T. & Saparov, A. Progress in the Development of Chitosan-Based Biomaterials for Tissue Engineering and Regenerative Medicine. *Biomolecules* **9**, 470 (2019).

[2] Sultankulov, B., Berillo, D., Kauanova, S., *et al.* (2019) 'Composite Cryogel with Polyelectrolyte Complexes for Growth Factor Delivery', *Pharmaceutics*, 11(12), p. 650. doi: 10.3390/pharmaceutics11120650.

[3] Jimi, S., Jaguparov, A., Nurkesh, A., Sultankulov, B. & Saparov, A. Sequential Delivery of Cryogel Released Growth Factors Accelerates Wound Healing and Improves Tissue Regeneration. *Front. Bioeng. Biotechnol.* **8**, 345 (2020).

Conference Presentations

[1] Bolat Sultankulov, Sholpan Kauanova, Sergey Mikhalovsky, Lyuba Mikhalovska, Dmitriy Berillo and Arman Saparov. *Macroporous Cryogel for Bone Regeneration.* Oral Speech BIT's 2 - International Biotechnology Congress-2018 (October 16-18, 2018 in Fukuoka, Japan);

[2] A. Saparov, B. Sultankulov, N. Mansurov, A Jaguparov and A. Altaikyzy. *A Novel Drug Delivery System for Tissue Regeneration*. Tissue Engineering & Regenerative Medicine International Society Meeting, Brisbane, October 2019 (Abstract);

[3] S. Jimi, B. Sultankulov and A. Saparov. *Growth Factors, Incorporated into Cryogel, Accelerate Regenerative Healing in Mouse Skin Wound Model*. Tissue Engineering & Regenerative Medicine International Society Meeting, Brisbane, October 2019 (Conference paper).

CHAPTER 2. LITERATURE REVIEW

This chapter highlights recent advances in CHI-based biomaterials in drug delivery, bone regeneration, and wound healing applications. CHI is the main component of the obtained cryogel scaffold evaluated in this dissertation and a short review of progress made in CHI-based scaffold in bone and skin regeneration is highlighting achieved results in this thesis.

Part of the work presented in this chapter was published in [1].

2.1 Efficacy of chitosan for wound healing

Skin regeneration is a complex process and consists of three phases: hemostasis and inflammation, tissue proliferation, and remodeling [28]. In other words, skin regeneration is a complex process involving blood products, extracellular components, secreted factors, and cells. [29]. Therefore, treatment of skin lesions involves dressing not only to ensure the physical protection of the wound but also to enhance healing, antimicrobial resistance, and minimize the development of scars. [30]. CHI has a very high hemostatic activity that is not dependent on the pathway of host coagulation [31] but depends on the molecular weight (MW) and DD of CHI [32,33]. The amount of amine groups has a direct impact on blood coagulation, where moderate DD (68.36 %) allows the mesh-like structure to form within CHI, thus promoting interaction with blood components, while higher DD results in stronger hydrogen bonds within CHI causing the formation of a crystalline structure with restricted ability to interact with red blood cells (RBC) [32–35]. Due to increased interaction between polyelectrolytes, higher MW could further increase the procoagulation effect [36,37]. Several CHI containing hemostatic products are available and approved by the United States Food and Drug Administration (FDA), such as Celox ®, HemCon ®, Axiostat ®, Chitoflex ®, and Chitoseal ® [38].

In addition to the hemostatic effect of CHI, it has been shown that CHI affects all stages of healing in different ways. CHI has been shown to induce neutrophil migration [39], neutrophil-like HL60 cells secret IL-8, a potent neutrophil chemokine in direct correlation with the N-acetylation level in response to CHI [40]. CHI has an immunomodulatory effect that is essential to wound healing and is DD-dependent [41]. Micro- and nano-sized CHI particles cause inflammasome formation by the macrophages [41–44]. In comparison, macro-sized CHI scaffolds inhibit the release of IL-1β and thus the formation of inflammasomes *in vitro* in mouse and human macrophages [45]. This allows the use of macro-sized CHI scaffolds when excessive inflammation occurs. CHI also affects growth factor expression by increasing early post-injury expression of TGF-β1 [46] and decreasing at a later stage by binding to anionic growth factors [47]. High DD CHI induces the proliferation of dermal fibroblasts, allowing the development of fibrous tissues and re-epithelialization [48,49]. CHI containing wound healing scaffolds could be produced as 2D (films and fibers) and 3D (gels and sponges) all with the different properties required for wound healing. [50]. Addition of antimicrobial agents may improve the antimicrobial effect of CHI. Complex CHI-cordycepine hydrogel with increased antimicrobial activity has recently been developed through a freeze-drying process without the addition of any cross-linking agents, with negatively charged cordycepine adhering to positively charged CHI chains. [51]. In another research, textile polyethylene terephthalate (PET) composed of layer-by-layer coated CHI was filled with chlorhexidine, thermal post-treatment improved the mechanical stability of the composite, which also improved the chlorhexidine release time up to 7 weeks [52]. CHI is often used as part of asymmetric membranes on its own or in combination with other natural polymers, typically in the underlying layer in contact with damaged skin [53]. Adding nanoparticles (NPs) to hydrogels is another strategy used in the preparation of biomaterials [20]. Recently developed triple-component nanocomposite film

containing CHI-silver-sericin loaded with high antimicrobial moxifloxacin against methicillin-resistant Staphylococcus aureus (MRSA) strains (clinical isolates) also promote rat wound healing and effective as commercial wound dressings [54]. The majority of collagen-containing CHI composite films have inherent properties to induce healing, but the major disadvantage is an allergic reaction to non-human collagen and therefore other safe substitutes are required. As a substitution human keratin-CHI UV-crosslinked membranes with improved mechanical properties show potential as a wound dressing [55]. CHI-chondroitin based polyelectrolyte complex exhibits an effective antimicrobial activity and cytocompatibility suitable for wound healing applications [56]. Also, positively charged CHI containing biomaterials may be treated with growth factors and cytokines to increase their efficacy in the treatment of wounds. Recently GM-CSF was loaded into CHI NPs which were prepared via the ionotropic gelation method using tripolyphosphate [57,58]. GM-CSF's loading efficiency was 97.4 % ±1.68 % with a continuous release of ~100 % over 48 hours, and *in vivo* results demonstrate that composites filled with encapsulated GM-CSF in CHI NPs induce greater closure of the wound compared to composite alone [57]. Nanofibers containing CHI NPs loaded with GM-CSF also showed accelerated wound closure [59]. CHI also could be modified with peptides for enhanced wound closure, as it was shown with CHI-peptide hydrogel containing Ser-Ile-Lys-Val-Ala-Val [60], *in vivo* results on mice show that applied hydrogel induces angiogenesis, expression of collagen and TGF-β1, inhibits expression of TNF-α, IL-1β IL-6 [61]. Sulfonation degree of CHI could also elevate its affinity to growth factors, for example, VEGF has higher affinity 2-N, 6-O-sulfated than to Hep [62,63].

2.2 Bone and Cartilage Regeneration

It is important to build not only a biocompatible and biodegradable scaffold while developing biomaterials for bone and cartilage regeneration, but porous material [22] promoting cell differentiation [64]. Biomaterials with these desirable properties cannot always be produced using just one polymer, so composite materials are manufactured or hybrid materials where a supporting scaffold can be added to satisfy the required mechanical properties [65]. CHI could be used to design biomaterials suitable for hard tissue regeneration. CHI scaffolds lack mechanical stability in a hydrated state and thus need extra modifications [66]. CHI causes apatite deposition [67–69] and this property has been used to promote the biomineralization of composite materials, for example, biomineralization of poly(ethylene glycol) diacrylate/CHI based hydrogel [53].

2.2.1 Bone

CHI mechanical properties are generally increased by the addition of hydroxyapatite (HA) due to its biological similarity to the inorganic bone portion [70]. Other composites with suitable mechanical properties were also designed and include nano-zirconia/CHI, nano-calcium zirconate/CHI, and strontium-modified CHI/montmorillonite composites [71,72]. Pre-osteoblast cells MC3T3-E1 have been shown to have significantly higher alkaline phosphatase activity, calcium deposition, and ECM synthesis when cultured on the CHI-graft-polycaprolactone copolymer surface compared to tissue culture treated with polystyrene (TCPS) surface [73]. Enhancement of mechanical properties of composite scaffolds is possible due to the polycationic structure of CHI which enables the design of PECs with polyanionic polymers [22,74]. It was shown that PEC based CHI/chondroitin/nano-bioglass composite material in addition to the accumulation of apatite increased

expression of type-1 collagen by MG63 osteoblast-like cells *in vitro* and enhanced osteointegration *in vivo* [75]. Increased ECM production, minimal inflammatory response, and enhanced bone regeneration of implanted CHI/gelatin scaffolds were shown in mice [76]. Biomineralization properties of CHI could be further enhanced by the addition of fucoidan [24,77] and bioglass [78]. Thermosensitive hydrogel based on CHI has been also developed but has some biocompatibility problems due to an increase in the amount of beta-glycerophosphate required for gelation at body temperature. In comparison to CHI, TEMPO-oxidized cellulose nanofibers induce faster gelation, good porosity with better biocompatibility *in vitro* and *in vivo* [79]. Osteointegration of metal implants could be increased by layering CHI on top of metal ([80,81]. Protection against corrosion could be also achieved by using CHI, polypyrrole/CHI composites synthesized through in-situ electrochemical polymerization in oxalic acid medium and coated on the surface of 316L SS implants has increased protection of metal against corrosion [82]. CHI has been utilized in 3D printing [83]. For example, CHI-HA hydrogels produced by thermal cross-linking reaction using glycerol phosphate disodium salt were successfully printed on extruder based bioprinter with increased osteogenic markers expression by seeded cells [84].

2.2.2 Cartilage

For modern orthopedics, regeneration of cartilage weakened by injury, disease (osteoarthritis), and degeneration arising from aging is an important task. Microfracture (MF), mosaicplasty (MO), autologous chondrocyte, and biomaterial implantation are methods used to regenerate cartilage [85]. A significant limitation is the absence of blood vessels in the cartilage tissue, thus, the main objective of tissue engineering is to build a biomaterial capable of stimulating cartilage regeneration under avascular conditions. [86]. Therefore, designed biomaterials made to

regenerate cartilage should be capable of promoting cell proliferation and differentiation [87,88]. The scaffold's microstructural, physicochemical, and biochemical properties should be able to provide a temporary template for cells and promote ECM synthesis required for the formation of cartilage tissue [89]. This means the scaffolds should be porous with interconnected pores, in addition to biocompatibility and biodegradability [87]. For the cartilage regeneration, 3D scaffolds such as hydrogels, fibrous materials, and foams/sponges are typical scaffolds [89]. Scaffolds usually comprise cells (differentiated chondrocytes and stem cells) and bioactive molecules (peptides, growth factors, and cytokines). In this regard, hydrogels have high water content, could support chondrogenesis, ability to implant without open surgery, offering in situ scaffold formation. The low mechanical properties of hydrogels (E ≈ 200 kPa) [85] can be resolved by using strong supporters that enhance hydrogel's mechanical stability[90]. CHI structure is close to endogenous sulfated GAGs, therefore provides a compatible microenvironment for chondrocyte proliferation, ECM synthesis, and chondrogenesis [86,88,91–93]. Chondrocytes cultured in CHI-alginate beats in comparison to alginate beads only secrete less inflammatory cytokines (IL-6 and IL-8) and increase cartilage ECM (hyaluronan and aggrecan) synthesis *in vitro* [94]. Chondrocytes cultured *in vitro* on carboxymethyl-CHI (CHI derivative) show reduced the inflammatory profile detected by reduced iNOS expression and upregulation of the anti-inflammatory cytokine IL-10 [95]. In another study, co-culture of the human infrapatellar fat pad (IPFP)-derived mesenchymal stem cells (MSCs) with the osteoarthritic chondrocytes after the addition of hyaluronic acid-CHI NPs resulted in the development of healthy chondrogenic differentiation [96]. 3D-printed CHI scaffolds support differentiation of human IPFP-MSCs cultured in chondrogenic media containing TGFβ3 and BMP6 into chondrocyte-like cells and the formation of cartilaginous like tissue *in vitro* [97]. The abundant presence of amino and sulfo groups in CHI allows its electrostatic

interaction with collagen [98], collagen-CHI hybrid scaffolds show improved mechanical properties, with a good porous structure similar to cartilage [99]. Mechanical properties of collagen-CHI scaffolds for cartilage regeneration were further improved in combination with PLGA as a bi-layer [100]. CHI blended with silk fibroin has also demonstrated the potential for cartilage regeneration [101,102]. CHI in the form of fiber with a diameter of 300 nm produced by the electrospinning method has shown efficacy for inducing collagen II/collagen I expression by bovine chondrocytes, making it approximately 2-fold higher when compared to other sponge-like scaffolds [103]. A new type of supermacroporous scaffold made by cryogelation is getting a lot of attention. Supermacroporous (85–100 μm pore diameter) CHI-agarose-gelatin cryogels made by the cryogelation method possess good mechanical properties with a compression modulus approximately 44 kPa [104]. In vivo implantation of CHI-agarose-gelatin cryogels for the repair of subchondral cartilage defects in a rabbit animal model using have demonstrated the formation of hyaline cartilage with the absence of hypertrophy markers by the fourth-week post-implantation [105]. Biochemical pathways reveal that mTOR/S6K is activated by CHI films in human bone marrow mesenchymal stem cells which leads differentiation into chondrocyte-like spheroids *in vitro* [106]. The advantages of CHI for skin, bone, and cartilage regeneration are highlighted in Figure 2.

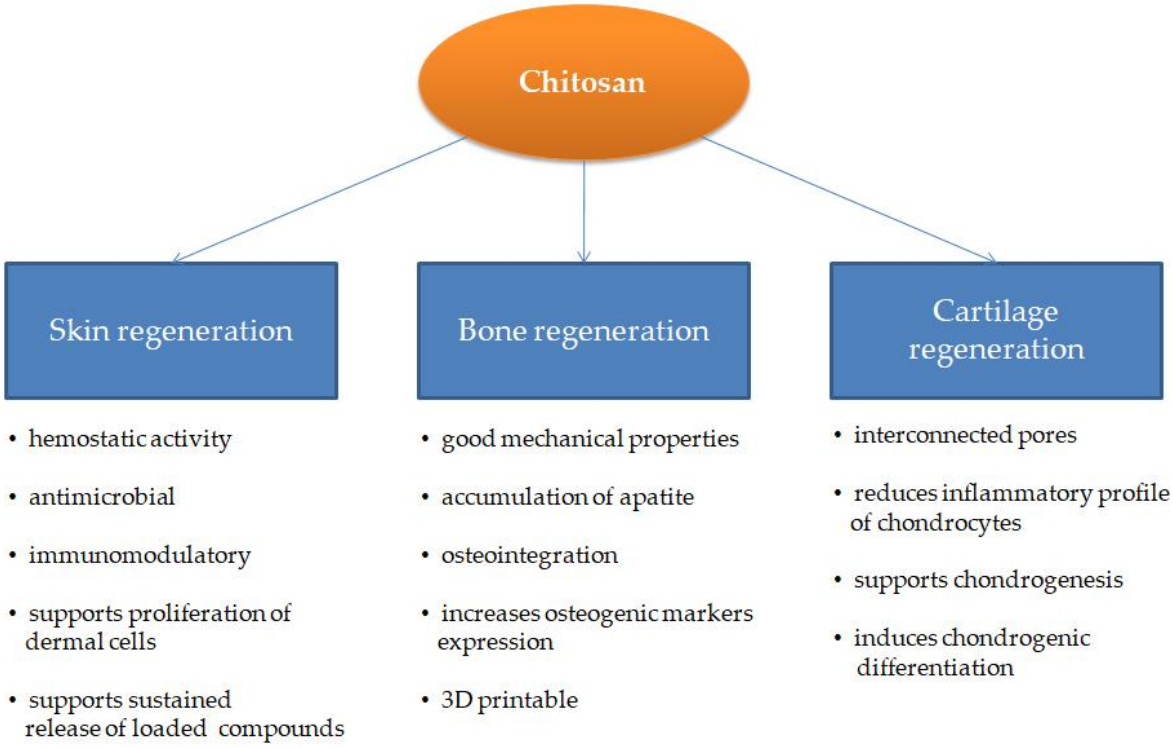

Figure 2. Fundamental rational of chitosan usage for skin, bone, and cartilage regeneration.

2.3 Chitosan for Drug Delivery

CHI found its use in drug delivery applications. It is biodegradable and degraded by mucosal tissue lysozyme [107] and chitinase produced by intestinal flora [108]. Low solubility under physiological pH possesses some limitations, however, it could be used for oral drug delivery due to increased solubility under acidic conditions. Due to its mucoadhesive nature [109], CHI has been used as a vehicle for the delivery of drugs to the nasal [110], ocular [111], buccal [112], and pulmonary tissues [113]. CHI is used for drug delivery in the form of nano/micro-particles that are synthesized by emulsion, coacervation/precipitation, ionic gelation, reverse micellar methods, etc. [15]. CHI is usually modified to increase the solubility of CHI under physiological conditions and includes quaternization, alkylation, acetylation, carboxymethylation, CHI/polyol salt combinations, synthesis of N-trimethyl chitosan, generation of sugar-

bearing chitosan, conjugation with polyethylene oxide, generation of glycol-CHI, etc. [15,114]. Amphiphilic CHI derivatives are used for the encapsulation of hydrophobic substances [115]. CHI derivatives could form micelles in aqueous media via the addition of alkyl groups (hydrophobic) to CHI moiety and the addition of succinyl groups (hydrophilic) such as succinyl to the amino groups [116]. Micelle-forming CHI derivatives, such as N-succinyl-N'-octyl chitosan (SOC), N-octyl-N-trimethyl chitosan (OTMC) and N-octyl-O-sulfate were studied to deliver doxorubicin (DOX), hydroxycamptothecin (10-HCPT), paclitaxel for tumor-targeted therapy and demonstrated increased encapsulation [115].

CHI NPs could be produced by the emulsion method and were studied for the delivery of proteins and peptides demonstrating high loading efficiency and sustained release [117]. However, CHI NPs production includes the use of cross-linking agents (tripolyphosphate, GA, and genipin) which could affect the biological activity of loaded proteins [118]. This could be prevented with the use of coacervation/precipitation, ionic gelation, polyelectrolyte formation, spray drying, and supercritical fluid drying methods [119]. For example, CHI microspheres carrying recombinant human interleukin-2 have been prepared by the coacervation/precipitation method [120]. PECs are also could be used, for example, CHI-Hep complexes can bind growth factors and cytokines [121–125]. CHI-Hep PECs were also shown to be effective than plasmid DNA in delivering siRNA against VEGF in human retinal epithelial cells (ARPE-19) demonstrating 2-fold higher transfection efficiency [126]. CHI could be modified to deliver growth factors and cytokines [127]. Hep and heparan sulfate like properties were given to CHI via the addition of sulfate group, importantly, this modification didn't affect the intrinsic antimicrobial properties of CHI [128]. Sulfated CHI can bind and protect FGF-2 [129], BMP-2 [130] from proteolytic cleavage [131], showing a higher affinity that Hep [132].

In 1995 CHI was used as a plasmid delivery vehicle [133] and explored as a non-viral gene delivery system [15,134]. Today, CHI is widely used in the delivery of siRNA [135] and miRNA [136,137]. Ionic gelation and [138,139] coacervation [140,141] are the main methods for preparing CHI for gene delivery. The polycationic nature of CHI allows the formation of PECs with not only negatively charged nucleic acid molecules [142,143], but also with negatively charged cellular membranes, this results in increased uptake efficiency [144]. Table 1 summarizes the application of CHI and its derivatives for drug delivery.

Table 1. Chitosan and chitosan derivatives for drug delivery applications.

Modification	Type	Application	Ref.
N-succinyl-N'-octyl chitosan (SOC) 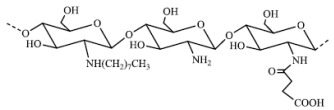	Forms micelle in aqueous media with hydrophobic and hydrophilic moieties	A sustained release of doxorubicin (DOX), 10-Hydroxycamptothecin (10-HCPT)	[116,145] 1.
		Macrophage engulfed SOC-paclitaxel (PTX) particles for tumor-targeted therapy	[146]
N-octyl-N-trimethyl chitosan (OTMC) 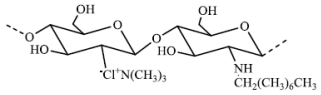	Forms spherical micelles in aqueous media with hydrophobic and hydrophilic moieties. Cytotoxic due to exposed positive charge	Increases solubility of 10-HCPT 80,000-fold	[147]
		Coated with two anionic polymers, heparin sodium and sodium carboxymethyl cellulose with decreased cytotoxicity, enhanced the delivery and tumor targeting of PTX	[148]
N-octyl-O-sulfate chitosan 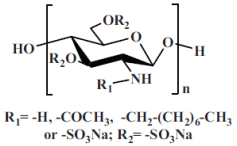 R_1= -H, -$COCH_3$, -CH_2-$(CH_2)_6$-CH_3 or -SO_3Na; R_2= -SO_3Na	Forms micelle in aqueous media with hydrophobic and hydrophilic moieties	Enhancement on oral absorption of PTX	[149,150]
		Optimal cytotoxicity to multidrug resistance HepG2 (HepG2-P) cells	[151] 2.
		Increases stability of docetaxel (DTX) liposomes *in vitro* and *in vivo*	[152]

2-[phenylhydrazine (or hydrazine)-thiosemicarbazone]-chitosan	Antioxidant activity higher than ascorbic acid	Possible use in pharmaceutical and food industries.	[153]
(Ser-Ile-Lys-Val-Ala-Val) peptide-modified chitosan	Hydrogel	Skin substitutes for wound closure in mice	[154]
Galactosylated chitosan (GC)	NPs	Calcium leucovorin loading for colon cancer cell-targeted drug delivery	[155]
O-palmitoyl chitosan (OPC)	Liposomes	Increased intestinal absorption of OPC containing liposomes	[156]
HA/CHI	NPs	CD44-targeted delivery of Everolimus	[157]
CHI coated with HA	NPs	Delivery of anti-angiogenic siRNA on CD44-positive tumor endothelial cells	[158]
CHI loaded with resveratrol loaded DMAEMA-HEMA-block-(DEAEMA-FMA NPs	Hydrogel	Mucoadhesive, resveratrol release for inflammatory bowel disease, Crohn's disease	[159]
PEGylated CHI	NPs	Methotrexate (MTX) plus pemetrexed (PMX) delivery for the lung cancer	[160]
CHI-DNA (pcDNA3.1-VP1 plasmid encoding VP1 capsid protein of	Polyelectrolyte	Intranasal CHI-DNA vaccine	[161]

Coxsackievirus B3)

2.4 SUMMARY

This Chapter described the intrinsic properties of CHI and its use in biomedical applications. CHI as a natural polymer is actively used in tissue engineering and regenerative medicine on its own as well as in combination with other polymers. CHI has a natural capacity to promote tissue regeneration, in addition to its appropriate mechanical physico-chemical properties. Active research on improving CHI-containing scaffolds for wound healing, bone, cartilage regeneration, drug delivery is ongoing. Further work on CHI-containing scaffold preparation through 3D printing and cryogelation methods would accelerate the application of CHI in biomedicine. As part of any material, CHI could introduce valuable properties such as antimicrobial activity, mucoadhesive property, and biocompatibility which are required for biomedical use. Research on CHI and combinations of its use with other polymers will show even greater prospects and properties for biomedical applications of this particular polymer. The following Chapter will describe novel CHI-based PEC cryogel material resulted from the work accomplished in this thesis for bone regeneration applications.

CHAPTER 3. PEC-BASED CRYOGEL FOR BONE REGENERATION APPLICATION

This Chapter provides an evaluation of obtained cryogels for bone regeneration applications. Includes physico-chemical characterization of obtained cryogel material and its biological activity. The work presented in this Chapter was published in [2]. Macroporous scaffolds made up of CHI, HA, Hep and polyvinyl alcohol (PVA) were prepared by cryogelation using as a GA cross-linker. The addition of PVA to the reaction mixture slowed the formation of a PEC between CS and Hep which allowed for more thorough mixing and led to the development of the homogeneous matrix structure. The freezing of the CHI-HA-GA and PVA-Hep-GA mixture results in the development of a non-stoichiometric PEC between oppositely charged groups of CHI and Hep, allowing more efficient immobilization of the bone morphogenic protein 2 (BMP-2) due to electrostatic interactions. The obtained cryogel matrix, loaded with BMP-2, has been shown to stimulate differentiation of rat bone marrow mesenchymal stem cells (rat BMSCs) into the osteogenic lineage. Rat BMSCs attach to BMP-2 loaded cryogel and express osteocalcin *in vitro*. A composite cryogel with PEC may have a high potential for bone regeneration applications.

3.1 INTRODUCTION

. Bone regeneration is a complex and continuous process happening in the human body all the time [162]. Bone resorption and bone formation are the core processes in bone regeneration and disbalance in one of them could lead to bone disorders such as osteoporosis [163]. Osteoclasts are a type of bone cell which are derived from macrophages and responsible for bone resorption [164] Initially bone resorption is initiated by osteocytes, which are the most abundant cells in the bone and responsible for the initiation of bone resorption via RANKL expression [165]. Elevated RANKL

initiates the attraction of osteoclasts which further attracts osteoblasts to the injury sites [164]. The process is complex and includes different pathways where hormones, small molecules, vitamins and cytokines play the major roles [162]. One of the main molecule implicated in bone remodeling is BMP-2. Usually, BMP-2 is released from the bone matrix during osteoclast initiated bone resorption [166] and differentiates mesenchymal stem cells into osteoblast-like cells. Moreover, BMP-2 released by differentiated osteoblasts also induce survival and differentiation of osteoclasts, however only on RANKL expressing cells [166]. This is just a small part of biochemical pathways that are implicated in the complex process of bone remodeling, where bone regeneration is just one part of a life-long continuous process. BMP-2 belongs to the TGF-beta superfamily of growth and differentiation factors which play an important role in stem cell differentiation [167]. The addition of BMP-2 induced ectopic bone formation in the animal model and human model [168] and is FDA approved growth factors. The role of BMP-2 is still debated, especially its role in osteogenic differentiation of human mesenchymal stem cells [169]. It is generally accepted that BMP-2 increases the expression of Runx2 transcription factors which activates a group of genes required for osteogenic differentiation of stem cells [170]. Based on this observation we used BMP-2 as the main growth factor which will be loaded onto developed cryogel.

Bone regeneration is one of the most active areas of regenerative medicine and bone fractures are the most common organ injuries, particularly in the aging population In congenital bone defects, tumors, and infections, bone restoration is also required [15]. Critical size defects require large-scale surgery and in this case autografting is accepted as a gold standard treatment due to its osteogenic, osteoconductive, and osteoinductive potentials [171]. However, associated pain and morbidity from autografts, shortage of allografts, rejection issues require the development of alternative methods. Tissue engineering is a combination of engineering and biology

to create biomaterials and could be used for bone regeneration [172]. As a result, the development of a variety of natural and synthetic polymer-based materials and methods for the production of functionally active scaffolds are underway [173].

To replicate or rebuild living tissues, tissue engineering uses engineering methods and biological concepts [174]. Developing safe and efficient biomaterials in this respect plays a major role in this area of research. Increased demand for materials that could be used to regenerate tissues and organs stimulated research into the production of synthetic and natural polymers based biomaterials [125,173,174]. During the design of bioactive scaffolds, it is necessary to mimic the three-dimensional structure of the target tissue's extracellular matrix (ECM), which will be able to provide structural support and sustain cell proliferation, adhesion, differentiation, and biodegradation in a reasonable period to enable replacement with the native ECM [175].

Hydrogels are usually studied in soft tissue regeneration because of properties such as injectability, the formation of a three-dimensional network, and the capacity to encapsulate cells [176,177]. Despite these benefits, the nanoporous nature of hydrogels restricts proper vascularization as well as the movement of cells and nutrients to some extent, thereby reducing cell viability [177]. Cryogels are good alternatives to hydrogels and are easily made by physical or chemical crosslinking under freezing conditions [178–180]. A cryogel can be formed with pores of different sizes and increased interconnectivity through regulated freeze-thaw cycles. Cryogels made from natural polymers have a macroporous structure and are excellent candidates for bone regeneration due to their good mechanical properties. [180]. Crosslinking reactions of cryogel precursors occur at freezing temperatures, resulting in the formation of water ice crystals which after thawing results in highly porous and interconnected structures [178,181].

Because of CHI's biocompatibility and biodegradability, natural CHI scaffolds are promising structures for bone regeneration [7]. Bone consists mainly of an extracellular collagen matrix containing ~90% type I collagen, mixed with HA ($Ca_{10}(PO_4)_6(OH)_2$) crystals. The compact bone comprises an average of 70% calcium salts and a 30% matrix [182,183]. It has been shown that mineralized scaffolds support osteogenic activity and overall bone formation [184]. HA assists in imitating the extracellular natural bone matrix (ECM), providing a native chemical and physical structure for the formation of new bone. Increasing the rate of HA accumulation during bone tissue regeneration is beneficial [74]. Moreover, HA is considered to be biocompatible and osteoconductive and is commonly used for many orthopedic applications, including bone fillings and implant coatings [185]. Another major problem to be addressed when designing a scaffold appropriate for bone regeneration is the ability of the scaffold to promote vasculogenesis, which can be achieved either by immobilizing growth factors or by adding substances with an inherent capacity to bind growth factors [186].

The main focus of this thesis is the development of a one-step preparation method for Hep containing biologically active composite cryogel. Protonated amino groups of CHI form PEC immediately with sulfo and carboxyl groups of Hep, thereby reducing the possibility of mixing and obtaining a homogeneous solution for cryogel production. There are a limited number of studies directly related to cryogel scaffolds based on PEC, but extensive work has been done on PEC based on hydrogel, particularly containing CHI [9]. Researchers were able to obtain CHI-Hep PEC by blending and subsequent crosslinking with GA [187]. The possibility of preparing a biocompatible PEC cryogel with the internal porosity of walls composed of CHI, gelatin, and dextran dialdehyde was shown [22]. In this dissertation, CHI-PVA-Hep-GA biocompatible PEC cryogel was obtained, internal porosity of the walls as a sign of PEC was shown [22,188]. The key hypothesis of the current study is that the

incorporation of Hep into CHI-PVA cryogel allows BMP-2 to be immobilized without further chemical modifications of a growth factor or cryogel. Figure 3 shows the PEC cryogel structure and chemical interactions between each component. Biocompatible with the cells, obtained cryogel possesses biological activity and induces the differentiation of rat BMSCs into osteogenic lineage by sustained release of BMP-2.

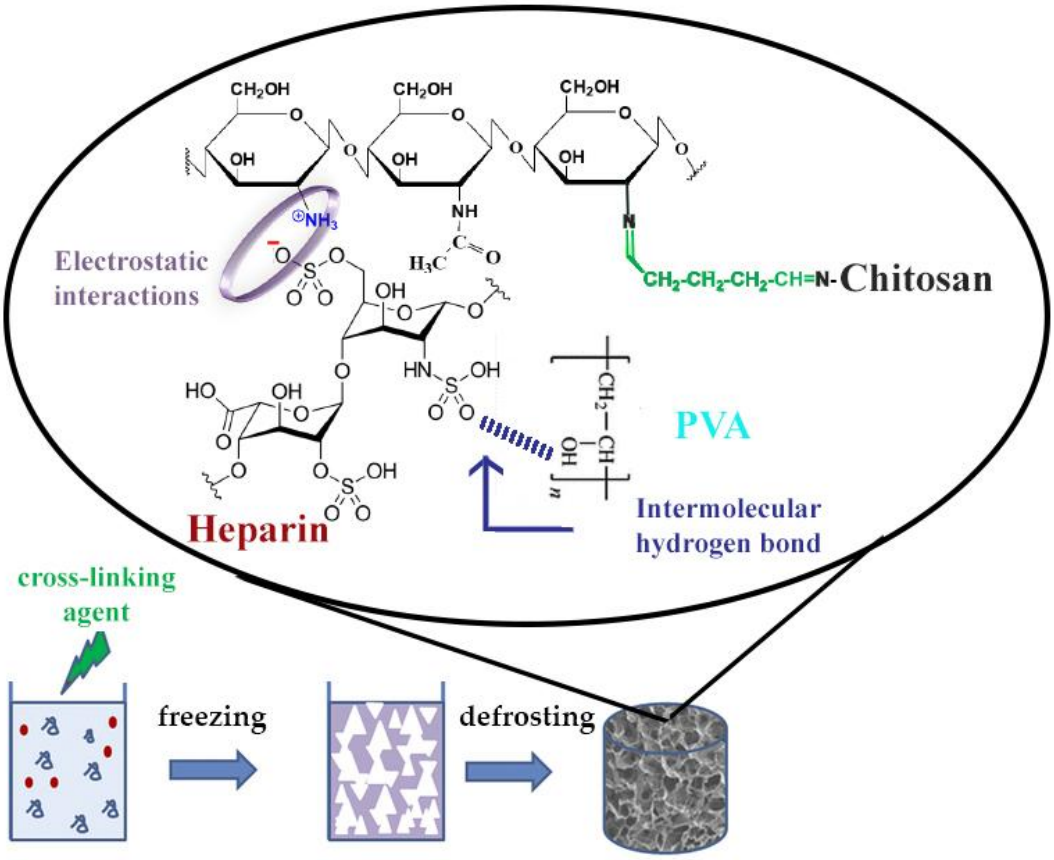

Figure 3. Schematic representation of polyelectrolyte complex (PEC)-based cryogel synthesis demonstrating interactions between cryogel components.

3.2 MATERIALS AND METHODS

CHI (low viscosity), GA (25% v/v) and polyvinyl alcohol were purchased from Fisher, UK; Leucine, Dulbecco's modified eagle's medium-high glucose (DMEM), dexamethasone, β-Glycerophosphate disodium salt hydrate 98%, ascorbic acid-2-phosphate, lysozyme, 75 μm HA particles, fetal bovine serum (FBS), rhodamine B were purchased from Sigma-Aldrich (St. Louis, MO, USA); Hep ≥150 I.U./mg (ACROS Organics, USA), antibiotic cocktail (penicillin and streptomycin Gibco®, MA, USA). rhBMP-2 (Sigma-Aldrich, St. Louis, MO, USA) and rhBMP-2 ELISA kits (R&D Systems, USA), Alizarin Red (ACROS Organics, USA), MTT Cell Growth Assay Kit (CT01, Merck, USA), mouse monoclonal osteocalcin antibody [OCG3] (ab13420, Abcam, UK), goat anti-mouse IgG, Superclonal™ Recombinant Secondary Antibody, Alexa Fluor 488 (Thermo Fisher, USA).

3.2.1 Synthesis of composite cryogels

CHI of 2% w/v was dissolved in 1% v/v acetic acid at room temperature for 1 hour at a magnetic stirrer. HA (20% w/v) was added into the ready CHI solution (5 ml) and mixed by stirring until a clear white solution was formed. The solution of the two remaining ingredients, Hep (2.5 ml with a concentration of 1 mg/ml) and PVA (2.5 ml) was made in deionized (DI) water. PVA was dissolved in DI water (5% w/v) under prolonged heating at 80 °C until a clear solution was obtained. Both CHI/HA and Hep/PVA ready solutions were kept on ice all the time during the experiments. CHI/HA (5 ml) with a Hep/PVA solution (5 ml) solutions were mixed to form a cryogel solution. The final concentrations of CHI, HA, PVA, and Hep in the final solution were 1%, 10%, 1.25%, and 0.25 mg/ml (unless indicated otherwise). After the addition of ice-cold GA (0.5% (v/v)) into the cryogel solution, the mixture was stirred for 10 seconds, and 0.3 ml of the final solution was quickly transferred into special

glass tubes (d=7 mm). Glass tubes were placed into a cooling chamber (Arctest) at −12 °C for 12 hours. After incubation, the tubes were removed, and cryogels were thawed at room temperature and washed at least 3 times with DI water. After that cryogels were incubated with 2% glycine for 12 hours. Glycine blocks unreacted aldehyde groups in cryogel [189]. Ready cryogels were washed with DI water and freeze-dried until use. Control cryogels (2%CHI-10%HA) were also prepared.

3.2.2 Swelling properties of cryogels and porosity

Freeze-dried cryogels were sliced into small discs (n =3, d=7 mm, 2 mm thickness), weighed, and placed into DI water. At different time-points (1/3 min, 2/3 min, 1 min, 1 min 20 sec, 1 min 40 sec, 2 min, 1 hour), the weight of cryogel samples was recorded. The swelling degree was determined according to the following equation:

$$\text{Swelling degree} = (m_{swollen} - m_{dry}) / (m_{dry}) \quad (1)$$

The relative porosity of cryogel was estimated according to water uptake experiments [190]. Equilibrium reached cryogels were weighed (swollen cryogels, $m_{swollen}$, g) then, swollen cryogels were squeezed to remove excess water and weighed again ($m_{squezzed}$, g). Estimated porosity was estimated according to the equation:

$$\text{Porosity (\%)} = ((m_{swollen} - m_{squezzed})/(m_{swollen})) \times 100 \quad (2)$$

3.2.3 Mechanical testing

Texture Analyser TAXT Plus (Stable Micro System, UK) was used to measure the compressive moduli of the cryogel cylinders at room temperature (with a 5N load cell). All measurements were done on swollen cryogel cylinders. 5N load was used to compress cryogels at the rate of 0.05 mm/s. The compressive Young's modulus was calculated from <10% strain, at least 5 measurements were made.

3.2.4 *In vitro* degradation

Cryogels were sterilized in 70% ethanol solution, washed with DI water, and freeze-dried before use. The degree of degradation (α(%)) was calculated by comparing the initial freeze-dried weight of cryogels (m_i - initial mass in mg) to freeze-dried weights at different time points after incubation in PBS at 37 °C for 1, 2 and 4 weeks. At each time point, the freeze-dried weight of cryogels was recorded (m_f - final mass in mg). α(%) was calculated according to the equation:

$$\alpha(\%) = ((m_i - m_f)/ m_i)) \times 100 \quad (3)$$

3.2.5 Rheological analysis

HAAKE™ RheoStress™ 1 Rheometer (Thermo Scientific, UK) with a 0.5 mm gap between the cone and plate was used to measure the flow behavior and viscoelastic properties of the solutions. To determine the linear viscoelastic region of the tested gel solutions, amplitude sweep tests were performed at a constant frequency (ω) of 10^{-1} and an amplitude range of 0.1–100%. All experiments were performed at 25 ± 1 °C.

3.2.6 FTIR

Universal ATI, Perkin Elmer (Spectrum 650) FT-IR spectrometer, USA was used to conduct FTIR measurements. Mortar and pestle crushed freeze-dried cryogels were prepared for FTIR spectroscopy. FTIR spectra were obtained in the range of 4000 - 650 cm^{-1} during 64 scans, with 2 cm^{-1} resolution, using diffuse reflectance mode.

3.2.7 Microscopy

Optical microscopy (EVOS FL Auto 2 Cell Imaging System, USA), Confocal Laser Scanning Microscopy (Carl Zeiss, LSM 780, Germany) and Scanning Electron

Microscopy (Jeol, JSM-IT200 InTouchScope™, Japan) were used to visualize the porosity and internal structure of obtained cryogels. Cryogel slices (1 mm thick) were stained with 50 mM Rhodamine B (Sigma-Aldrich, USA) for 30 minutes before taking images with CLSM. Excitation and emission wavelengths were chosen according to the manufacturer's instructions. Freeze-dried slices of cryogels without coating were used for SEM imaging. Images were taken at variable accelerating voltage and magnifications.

3.2.8 Release of BMP-2 from cryogel matrix

Cryogel slices (n=3, d=7 mm, 2 mm thickness) were incubated with 20 ng/ml rh-BMP-2 overnight at room temperature and 50 rpm. After incubation, cryogels were transferred to the tube with fresh PBS (1 ml). Supernatants were collected at different time points (days 1, 7, 15 and 30), with fresh PBS added each time. ELISA assay (R&D, USA) was used to measure loading efficiency and release kinetics of BMP-2 by analyzing collected supernatants.

3.2.9 MTT Assay

Powders of freeze-dried CHI-PVA-HA-Hep-GA cryogel slices (n=3, d=7 mm, 2 mm thickness) were previously neutralized with 50mM sodium borohydrate were incubated in 1 ml growth media (10% FBS, DMEM, 1% penicillin/streptomycin) for 6 hours. After incubation, the supernatants were collected by centrifugation at 6000 × g for 10 minutes and sterile filtered through a 0.22 μm to prepare cryogel extract solution. NIH/3T3 cells at concentration 5×10^4 were seeded into a 96-well plate and incubated at 37 °C in a humidified 5% CO_2 atmosphere for approximately 18 hours until reached required confluency. 10 μl of supernatant was mixed with 90 μl of fresh media and added into each well with the NIH/3T3 cells. Culture media only was

included as a negative control. The cells were further incubated with cryogel extracts for 24 hours. After incubation, the cell viability of NIH/3T3 was measured using MTT Cell Growth Assay Kit (CT01, Merck, USA) according to the manufacturer's instructions.

3.2.10 Rat BMSCs differentiation into osteogenic lineage

Cryogel slices, (n=5, d=7 mm, thickness = 2 mm) were inactivated with 50 mM sodium borohydrate (NaBH4) and cut into 4 pieces. And then incubated overnight in 1 ml of BMP-2 solution (1μg/ml). Rat BMSCs passage 5 were used to assess BMP-2 release from cryogels. BMSCs cells were seeded (1×10^5 cells per well in a 24-well plate) in osteogenic media (OS media). The OS media was prepared and composed of DMEM, FBS 10%, 50 μg/ml ascorbic acid, 10 mM β-glycerophosphate, 10 nM dexamethasone. To assess the effect of BMP-2 released from cryogels 3 groups were formed: cells cultured in osteogenic media without cryogel (OS media), cultured in osteogenic media with cryogel pre-loaded with BMP-2 (OS-BMP media), and growth media only (DMEM, 10% FBS, 1% penicillin/streptomycin). On days 7, 14, and 21 days, cells were fixed with 2.5% GA for 30 min and washed three times with PBS (5 min incubation) before being stained with 1% Alizarin Red solution (pH 4.2) for 10 min. After the aspiration of the Alizarin Red solution, cells were washed with PBS and air-dried before taking color images (EVOS FL Auto 2 Cell Imaging System, Thermo Fisher Scientific, Bothell, WA, USA).

3.2.11 Rat BMSCs in cryogel

50 mM $NaBH_4$ neutralized cryogel slices (n=5, d=7 mm, thickness = 2 mm) were incubated overnight in 1 ml of BMP-2 solution (1μg/ml). Rat BMSCs passage 5 were seeded (1×10^5 cells per well in a 24-well plate) on top of cryogels and cultured for 2

weeks with OS media changed every 3. After 14 days, the cryogels were fixed with 2.5% GA overnight at +4 ^{0}C and washed 3 times × 10 min with PBS and then stained with mouse monoclonal osteocalcin antibody [OCG3] (ab13420, Abcam, UK) and goat anti-mouse IgG (H+L), Superclonal™ Recombinant Secondary Antibody, Alexa Fluor 488 (Thermo Fisher, USA) according to the manufacturer's instructions. After that osteocalcin stained cryogel slices were washed with PBS and stained with DAPI for 5 minutes and washed with PBS again (3 times). The negative control is cells grown on cryogel without BMP-2 in OS media. Images of stained cryogels were taken on a ZEISS LSM 880 confocal laser scanning microscope.

3.2.12 Statistical analysis

Data are represented as mean ± SD and all analysis has been done using an unpaired t-test. For experiments with more than 3 groups/time points, one-way ANOVA was used. p-value <0.05 was considered statistically significant. All experiments were carried out at least in triplicates (n=3) unless otherwise specified.

3.3 RESULTS

3.3.1 Cryogel Synthesis And Physico-chemical Characterization

Novel PEC-based CHI-PVA-HA-Hep-GA cross-linked cryogel was synthesized. As a control, cryogels without Hep were also included in this study to estimate the effect of each component on the physico-mechanical properties of cryogel. Cryogel synthesis was based on the polycondensation reaction of CHI-HA and PVA-Hep mixtures followed by GA crosslinking at −12 °C. Obtained composites had channels of large continuous interconnected pores (Figure 4a–d) with the surface area available for intermolecular binding. Microscopic imaging (CLSM and SEM) of cryogels (Figure 4) demonstrate high porosity and the PEC structure presence shown by porous cryogel walls (Figure 4d).

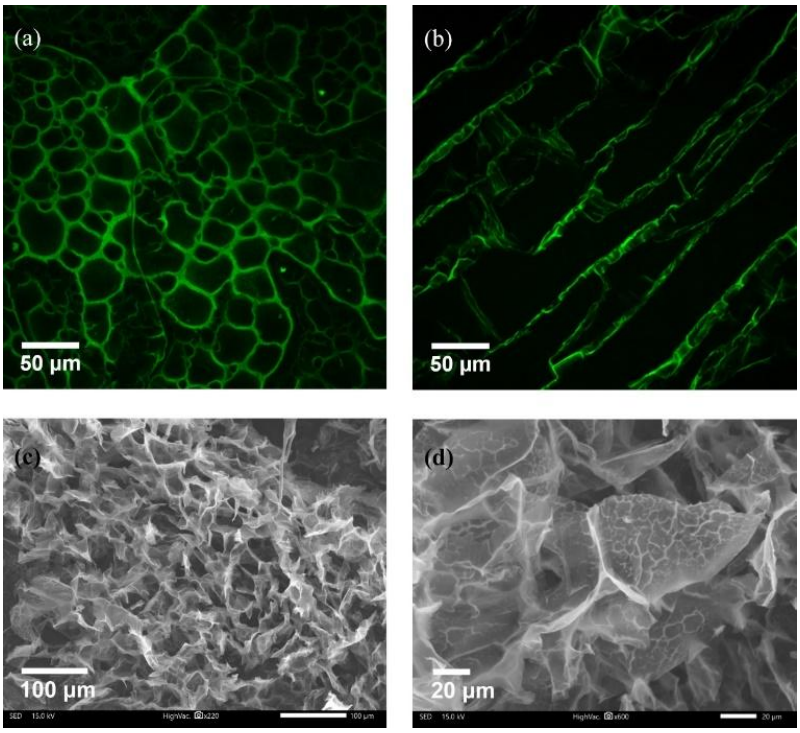

Figure 4. Microscopic images of obtained cryogel. Rhodamin B-stained CLSM images of cryogel (a,b). SEM images demonstrating porous structure (c) and porosity of the cryogel walls (d) representing PEC structure.

3.3.2 Mechanical and Rheological Properties

Representative stress-strain curves for each cryogel group are demonstrated in Figure 5a. A concave upward curve characteristic of elastomeric materials with large deformation has been observed. Classical CHI-HA-GA cryogels possess a significantly larger elastic modulus (2011.9 ± 328.80 kPa) in comparison to CHI-GA and PEC-based CHI-PVA-HA-Hep-GA (10.8 ± 0.47 kPa and 1085.2 ± 427.97 kPa, respectively) (Figure 5b). Addition of HA increases of the elastic modulus, which results in increased mechanical properties of the cryogels.

The flow behavior of CHI-PVA-HA-Hep solutions is between the pristine polymers (CHI and PVA) and represented on time-dependent viscosity charts of the different solutions (Figure 5c,d). The viscosity of CHI alone did not significantly change under applied shear stress, and interestingly the viscosity of the CHI-PVA-HA-Hep was predicted to be lower by the rule of mixtures [191] thus leaving questions on causes underlying of this behavior. The decreased viscosity at higher shear rates is caused by the shear itself, a high rate of stress causes the network of polymer mixtures to become more compact and triggers the formation of stochiometric PEC between the CHI and Hep polymers. This stochiometric PEC is more hydrophobic and thus tends to collapse, which explains a viscosity drop in the blend solution caused by the stress-induced additional interaction between available functional groups of CHI-PVA-HA-Hep. The viscosity values of other solutions are in line with their molecular weights. Multiple inflections were observed in the shear rate curve of the CHI-PVA-HA-Hep blend (Figure 5c) and could be explained by the formation and tearing of local structures. If more specifically as a result of the collapse and aggregation of PEC between CHI and Hep under applied stress.

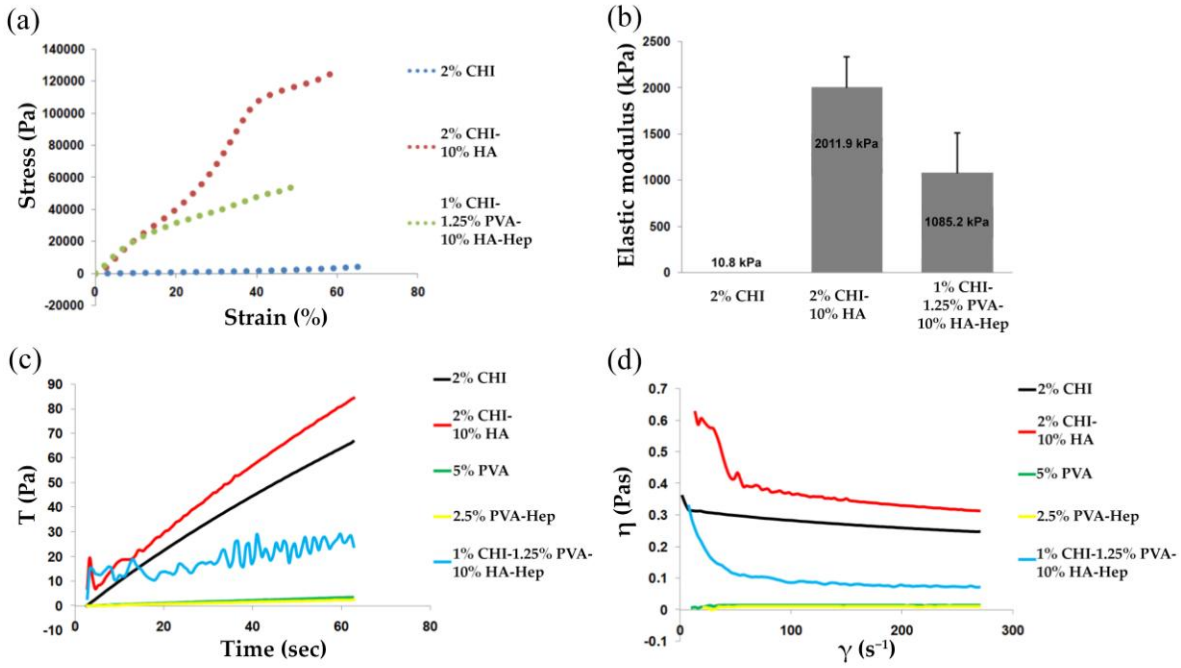

Figure 5. Physico-mechanical and rheological measurements. Stress–strain curves (a) and elastic moduli (b). Representative graph of viscosity measured at constant shear rate (c). Viscosity versus shear rate plot (d).

3.3.3 FTIR

FTIR spectra of initial components of CHI, PVA, Hep, HA, and the composite cryogel was analyzed and shown in Figure 6. The peak at 1635 cm^{-1} is the signature of CHI amide bond carbonyl stretching frequency [192]. 1550 to 1590 cm^{-1} shift in amino bond frequency is representing the reaction between the CHI primary amino groups and GA aldehyde. The peak at 3270–3400 cm^{-1} represents hydroxyl and amine groups of CHI [192], PVA, and Hep. CHI, PVA, and Hep functional groups were detected at 2929–2880 cm^{-1} (–C–H), 1548 cm^{-1} ($–NH_2$), 1404 cm^{-1} (the coupling of –C–N and –N–H [192], 1062 and 1026 cm^{-1} (–C–O), and 896 cm^{-1} (C–C ring of CHI and Hep). Schiff's base formation from 1633 to 1592 cm^{-1} is attributed to GA cross-linked composite cryogels. Frequencies CHI-PVA-HA-Hep cryogel functional groups are shifted and represent electrostatic interactions. Hep presence in the cryogel structure is

represented by a small intensity peak at 820 cm^{-1}(C–S–O group). The absorbance at 1230 cm^{-1} was attributed to asymmetric S = O bond is seen at 1230 cm^{-1} [193].

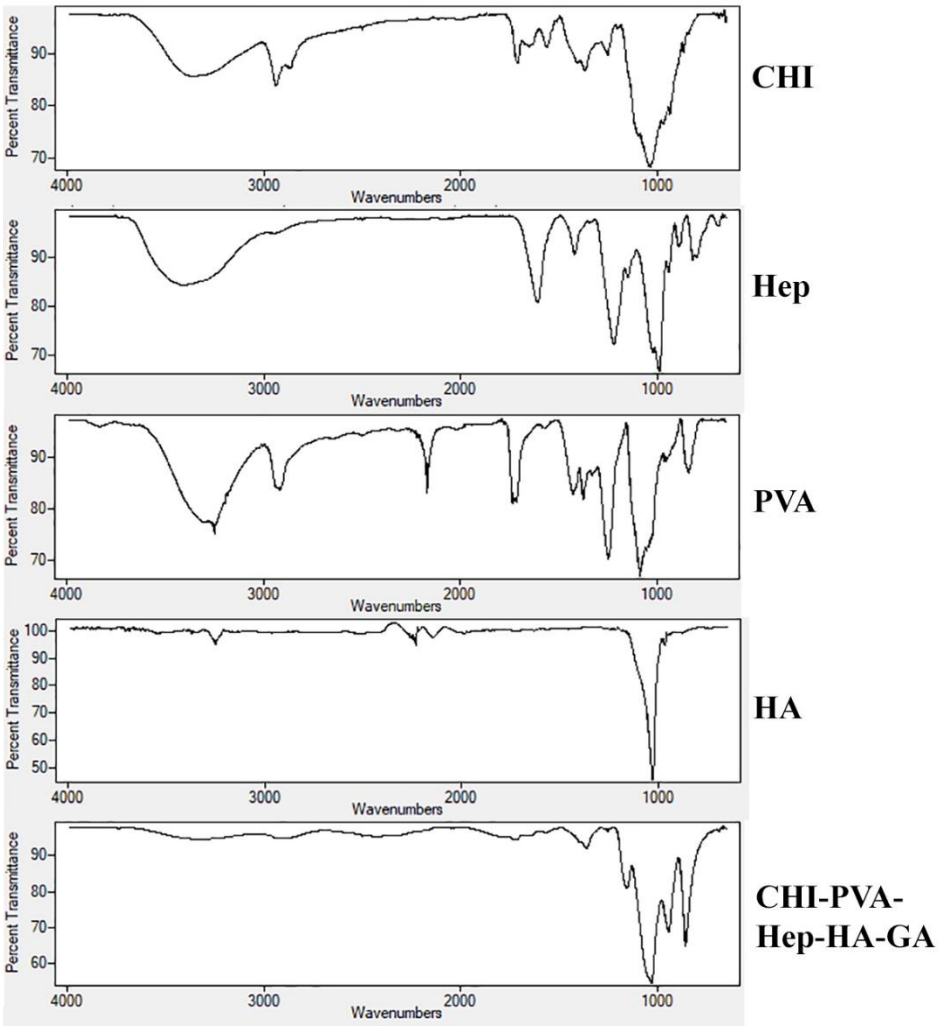

Figure 6. FTIR spectra. Functional groups of CHI, PVA, and Hep were detected at 2929–2880 cm^{-1} (–C–H), 1548 cm^{-1} (–NH_2), 1404 cm^{-1} (the coupling of –C–N and –N–H), 1062 and 1026 cm^{-1} (–C–O), and 896 cm^{-1} (C–C ring of CHI and heparin).

3.3.4 Degradation and BMP-2 release kinetics

In vitro degradation experiments in PBS for a period of 4 weeks (Table 2) revealed that PEC-based CHI-PVA-HA-Hep-GA cryogel is more stable and degrades slowly comparison to CHI-GA and CHI-HA-GA cryogels. According to published data non-

reduced Schiff's base cryogels are degraded in the range of 25% to 35% [22] which is in line with our observation.

Table 2. Degradation of obtained cryogels in saline and lysozyme solutions**.**

Sample	Degradation (%)			Degradation (%) in Lysozyme (10,000 U/mL)		
	1 Week	2 Weeks	4 Weeks	1 Week	2 Weeks	4 Weeks
CHI-GA	5.50 ± 0.71	11.93 ± 0.39	20.43 ± 0.18	19.48 ± 0.62	25.54 ± 0.40	41.22 ± 0.60
CHI-HA-GA	2.50 ± 0.70	4.68 ± 0.62	8.08 ± 0.41	8.65 ± 0.31	14.70 ± 0.35	22.55 ± 0.55
CHI-PVA-HA-Hep-GA	2.58 ± 0.60	5.20 ± 1.32	6.99 ± 0.16	10.22 ± 0.30	18.90 ± 0.95	25.61 ± 0.70

ELISA results show sustained and time-dependent release of BMP-2 (30 days) from obtained PEC-based cryogels (Figure 7a). BMP-2 loading efficiency was as high as ~83.2% and the total cumulative release of BMP-2 was found to be ~ 4.52%. This data follows the degradation cryogel matrix in PBS (Table 2) representing a high affinity of BMP-2. Toxicity experiments represented in Figure 7b, shows no cytotoxic effect of PEC-based cryogel extracts on NIH/3T3 cells after 24, 48, and 72 h incubation.

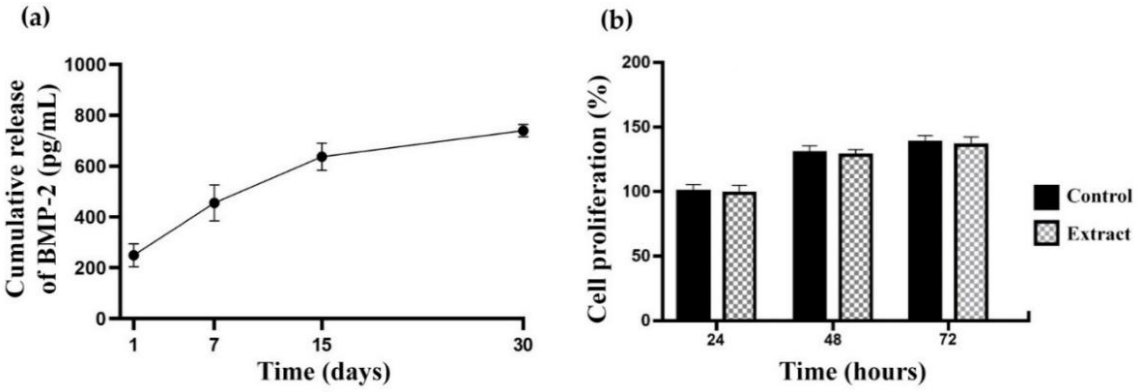

Figure 7. Release kinetics of loaded BMP-2 over 30 days (a) and cytotoxicity results (b). Measures were done in triplicates. Data is represented as mean±SD and all analysis has been done using an unpaired t-test.).

3.3.5 Osteogenic differentiation of rat BMSCs

Calcium deposition is a marker of bone mineralization caused by osteogenic differentiation of stem cells. Mineralization of rat BMSCs is visible on day 14. Rat BMSCs incubated in OS-BMP media (Figure 8a) mineralized by day 21 in comparison to the cells incubated in OS media only. However, the mineralization was not efficient as seen with commercial cell lines, possibly due to the use of primary cell lines which were heterogeneous and not enriched further against MSC markers using cell sorter or other techniques. Nevertheless, rat BMSCs grown for 2 weeks on BMP-2 loaded CHI-PVA-Hep-HA-GA cryogel (Figure 8b) are already expressing osteocalcin demonstrating no interference to osteogenic differentiation of stem cells.

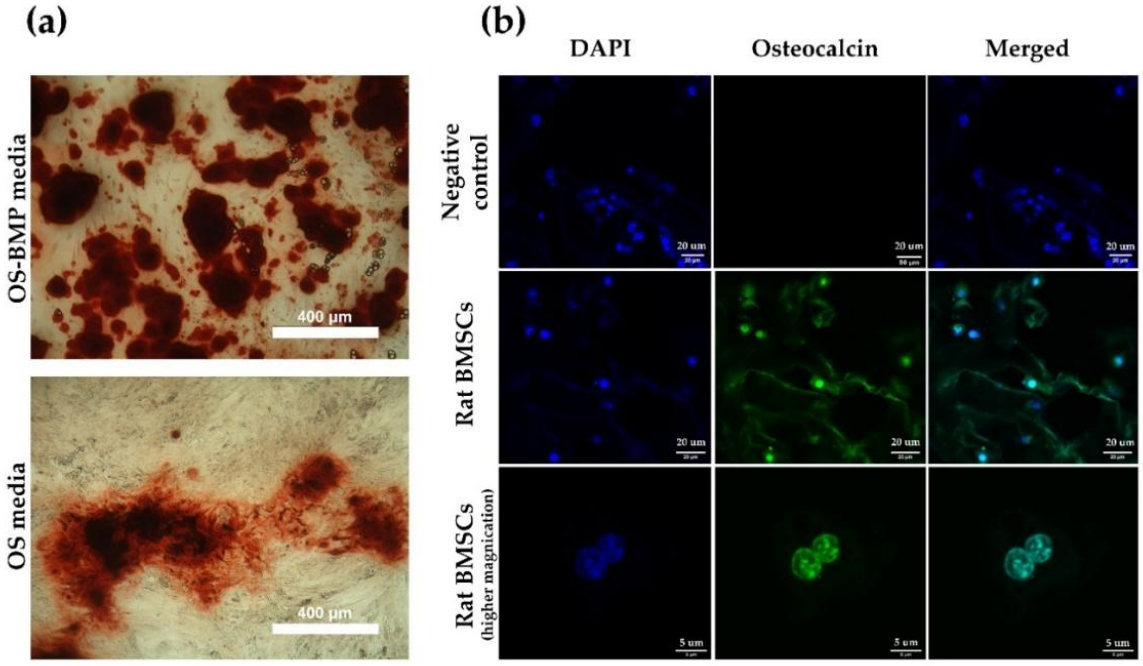

Figure 8. Osteogenic differentiation of rat BMSCs. Mineralized cells stained with Alizarin Red on day 21 (a). Differentiated rat BMSCs cultured on cryogel, stained with DAPI (blue) and anti-osteocalcin antibodies (green). Negative control—rat BMSCS grown on cryogel without BMP-2 in OS media.

3.4 DISCUSSION

The ECM plays an important role in tissue integrity and regeneration, and mimicking the target tissue matrix is important during the design of scaffolds for tissue engineering application. Cryogels have become a common material for tissue engineering purposes thanks to their macroporous structure, biocompatibility, and good mechanical properties [194,195]. The unique sponge-like structure of cryogels made them attractive to create scaffolds, bioreactors, and many other materials [179,196,197]. For example, cryogel bioreactors were used to produce antibodies, cell culture, separation and as a substrate for cryopreservation of cells [22,195,198–201]. More significantly, they have proven to be good candidates for scaffold engineering and show promise in tissue regeneration [180,202].

The objective was to develop PEC cryogel scaffold with the ability to bind growth factors and promote bone regeneration. Obtained PEC-based cryogel binds BMP-2 BMP-2 without any additional modifications of growth factor. Release kinetics and degradation experiments demonstrated an efficient loading of BMP-2 (~82.3%) and sustained release of bounded growth factor. As pointed in Table 1, CHI-PVA-HA-Hep-GA cryogel lost 7 % of its weight, which corresponded to the BMP-2 release of 4.52 % (700 pg). Heparin-binding sites are present in BMP-2 [203] which in addition to affinity also affects its biological activity [204]. Due to the PEC and heparin-binding sites, BMP-2 was released from the cryogel as a result of the natural degradation of the scaffold which is in line with obtained results. Experiments on BMP-2 release by control cryogels (results are not shown) was not conducted because the majority of growth factors failed to load onto cryogel materials. It is also known that HA has a natural ability to interact with BMP-2 via −OH, $-NH_2$, and −COO− functional groups of BMP-2 [205]. Therefore, HA was introduced to improve the strength and to increase the biocompatibility of the cryogel. Mechanical tests demonstrated that the addition of HA to CHI-PVA-Hep-GA cryogel significantly increased the elastic

modulus of cryogel (1085 ± 428 kPa) in comparison to other cryogel-based scaffolds produced for bone regeneration [206–212]. *In vitro* degradation rate of HA-containing cryogels confirmed a decrease, which is also supported by published data [208,213]. This could be explained by the removal of hydrolytically active groups by $NaBH_4$, in other words by reduction of Schiff's base groups [23]. Lysozyme is responsible for the *in vivo* degradation of CHI, which could be above 50% of its weight within 30 days [214,215], which is in line with our data. Microscopic imaging (Confocal and SEM images) of composite cryogels shows a highly porous structure with interconnective pores required for tissue engineering applications. Due to the positively charged nature of CHI and it is almost impossible to prepare a CHI-Hep cryogel by just mixing due to the instant formation of a PEC hydrogel. Through intensive experimentation it was found that the pre-mixing of Hep with PVA inhibits the rate of PEC formation when mixed with CHI, the explanation could be the formation of a non-stoichiometric interpolymer complex (IPC) between Hep and PVA at low temperatures. Decreased temperature is the best condition for the formation of hydrogen bonds. Rheological analysis has shown fluctuations in the flow curve of cryogel mixture, a sign of PEC formation. The significant decrease in viscosity of the solution in comparison to CHI and CHI-HA solutions is another signature of PEC which was also supported by the inflections on shear rate curves. These changes were not caused by HA, as the shear rate of CHI-HA is normal. We believe that fluctuations are the results of PEC formation and tearing between CHI and Hep. The detailed mechanism of PVA on PEC formation is out of the scope of the current study. However, IPC between PVA and negatively charged polymers were reported [216–218]. IPC between PVA-Hep is a possible cause of Hep's sulfo groups shielding from CHI which leads to an inhibited rate of PEC formation. The cryogelation of PVA-Hep and CHI-HA mixtures results in the formation of nonstoichiometric PEC between CHI and Hep as a result of the cryoconcentration effect. SEM images confirm the

presence of pores within cryogel walls, which was previously described as a PEC structure formation signature in cryogels [22].

Another important property of cryogels is their swelling kinetics. Composite cryogels swell within minutes with the high water absorption and reaching swelling equilibrium within 20-25 minutes. With the 9.5 ± 0.84 swelling ratio, 1085.2 ± 427.9 kPa average elastic moduli, CHI-PVA-HA-Hep-GA cryogel is a suitable substrate for implantation into the bone. CLSM imaging and staining of seeded rat BMSCs on BMP-2 loaded cryogel show good attachment, proliferation, and expression of osteocalcin by the cells *in vitro*, without any signs of cytotoxicity. BMP-2 in addition to the presence of the Hep-binding domain [167] loaded onto cryogel via electrostatic interactions with. *In vitro* experiments have shown that rat BMSCs differentiate into osteogenic lineage supported by BMP-2 released from cryogel in line with degradation rate. Further studies should explore the potential use of obtained novel PEC-based cryogel for bone regeneration *in vivo*.

3.5 SUMMARY

The possibility of a one-step preparation of a biologically active PEC-based cryogel scaffold for growth factor delivery, such as BMP-2 was evaluated. Novel PEC-based cryogel containing CHI and Hep is an appropriate scaffold supporting cell proliferation and differentiation. The potential application of the PEC-based CHI-Hep cryogels as a carrier of growth factors was demonstrated.

CHAPTER 4. EFFICACY OF OBTAINED CRYOGEL FOR WOUND HEALING APPLICATION

In this Chapter, *in vitro* and *in vivo* results of cryogel on enhancing wound regeneration will be discussed. Growth factors and cytokines loading and release kinetics will be assessed. Biological activity data will be discussed. To assess the *in vivo* effect of cryogel loaded with growth factors and cytokines, our cryogel sample was sent to Dr Shiro Jimi from Fukuoka University (Japan). As a result of our collaboration, the data present in this chapter is published in [27] and *in vivo* results are presented.

Healing of tissue from the injury depends on growth factors and cytokines that are secreted by different types of cells. To maximize healing and minimize side effects those factors should be released in a controlled manner at a specific time. Two growth factors (VEGF and FGF) and two cytokines (IL-10 and TGF-β) were incorporated onto novel PEC-based cryogel demonstrating sustained release kinetics and biological activity of factors *in vitro*. Used cytokines belong to inflammation modulatory factors and VEGF and FGF are well-known for the induction of wound healing. Biological activity of secreted factors released by cryogel was assessed using mouse mast cells (MC/9), mouse mammary gland cells (NMuMG), mouse fibroblasts (NIH/3T3), and human umbilical vein endothelial cells (HUVECs).

4.1 INTRODUCTION

Wound healing is a complex process and generally has four overlapping stages: hemostasis, inflammation, proliferation, and remodeling [219]. During tissue injury, affected cells release damage-associated molecular patterns which cause the formation of inflammasome which is associated with paracrine secretion of pro-inflammatory cytokines IL-1β and IL-18 [220,221]. Activated platelets secrete clotting

factors and facilitate matrix production required for migration of inflammatory cells into the damaged area and as well as secrete different paracrine factors such as platelet-derived growth factor (PDGF), IL-1, TGF-α and TGF-β implicated in tissue regeneration [221]. Neutrophils are attracted to the damaged site by pro-inflammatory cytokines and in addition to phagocytosis secrete proteases, reactive oxygen species, TNF-α, IL-1, IL-6, and chemokines that stimulate migration monocytes [222,223]. Monocytes start to differentiate into either pro-inflammatory macrophages or reparative macrophages [221]. Fibroblasts are also migrated and start to produce matrix metalloproteinases required for tissue remodeling which include newly synthesized ECM [223]. TGF-β which is highly present at the injury site cause differentiation of fibroblasts into contractile myofibroblasts required for wound closure [221,224]. Secreted VEGF and FGF induces endothelial cells proliferation and angiogenesis (proliferative phase), thus allowing oxygenation and nutrients delivery to the site of injury [225]. Re-epithelization is activated by EGF, TGF-α, and FGF via promoting epithelial cell migration and proliferation [226].

In the past few decades, different types of drug delivery systems based on polymers were developed to deliver secreted factors for wound healing applications [1,125]. Different biomaterials loaded with cytokines and growth factors have been studied. Hep-based hydrogels loaded with human EGF in addition to epithelialization, increases tissue granulation, and angiogenesis during wound healing [227]. Scaffolds incorporated with TGF-β reduce the production of pro-inflammatory cytokines TNF-α, IL-12, and MCP-1 and decrease leukocyte migration post-implant which enhances wound regeneration [228]. TGF-β in combination with anti-inflammatory factors IL-4 and IL-10 promotes a healing environment [229]. So, a combination of anti-inflammatory cytokines and pro-healing growth factors loaded into scaffold could accelerate tissue regeneration [230]. Based on widely published data on the healing effects of IL-10 and TGF-β as well as angiogenic properties of VEGF and FGF, these

secreted factors were chosen to assess their efficacy for wound healing application when loaded onto PEC-based cryogel. The main hypothesis is that sequential delivery of IL-10/TGF-β and FGF/VEGF by novel PEC-based cryogel would positively affect the inflammation and proliferation and thus accelerate tissue regeneration *in vitro* and *in vivo*.

4.2 MATERIALS AND METHODS

4.2.1 Preparation of Cryogel

Cryogels were prepared as previously described in the Materials and Methods section of Chapter 3, with one exception, no hydroxyapatite was added.

4.2.2 Cell Lines

Mouse mast cells, MC/9 (ATCC, USA), mouse mammary gland cells, NMuMG (ATCC, USA) and mouse fibroblasts, NIH/3T3 (ATCC, USA) were maintained in DMEM with 4.5 g/L glucose, 2.0 mM L-glutamine, sodium pyruvate, and sodium bicarbonate (Sigma, USA), supplemented with 10% fetal bovine serum (FBS) and 1% penicillin/streptomycin (Sigma, USA). Also, 4.0 mM L-glutamine, 10% Rat T-STIM with Con A (Corning, USA), and 0.05 mM 2-mercaptoethanol (Sigma, USA) were added to MC/9 cells and 10 μg/ml insulin (Sigma, USA) was added to NMuMG cells. Human umbilical vein endothelial cells (HUVECs) (Sigma, USA) were cultured in M199 (Sigma, USA) medium supplemented with 10% FBS (Gibco, USA).

4.2.3 Loading of secreted factors onto cryogel

Cryogel samples were sliced and sterilized as described previously. The following recombinant secreted factors were used: IL-10 (Gibco, USA), TGF-β1 (Gibco, USA), VEGF-165 (Invitrogen, USA), and FGF2 (Invitrogen, USA). All cryogel samples were

divided into 7 groups: 1) negative control - cryogel incubated with PBS; 2) cryogel incubated with 1 μg/ml of IL-10 and TGF-β1; 3) cryogel incubated with 0.3 μg/ml of IL-10 and TGF-β1; 4) cryogel incubated with 0.1 μg/ml of IL-10 and TGF-β1; 5) cryogel incubated with 10 μg/ml of VEGF-165 and FGF2; 6) cryogel incubated with 3 μg/ml of VEGF-165 and FGF2; and 7) cryogel incubated with 1 μg/ml of VEGF-165 and FGF2. At initial incubation, samples were incubated for four hours at room followed by centrifugation at 4,000 g for 10 min to remove unincorporated factors. After that, the cryogels were washed with PBS (3x times), dried and incubation at 37° C in PBS supplemented with 10,000 U/ml of lysozyme (Sigma, USA). To assess release kinetics, the supernatants were collected at 1, 3, 5, 7, and 10-day intervals and stored at -20 °C.

4.2.4 ELISA

ELISA was performed according to instructions provided by the manufacturer (All Invitrogen, USA). All measurements were done in duplicates at 450 nm (Mithras LB 940, Berthold, Germany).

4.2.5 Wound healing assay to assess FGF biological activity

CytoSelect 24-well Wound Healing Assay (Cell Biolabs, USA) was used to determine the biological activity of released FGF. All manipulations were done according to the manufacturer's instructions. 0.9 mm wound field inserts were placed into collagen-coated (50 μg/ml in 0.1 M acetic acid (Millipore, USA)) 24-well plate. 10 x 10^5 of NIH/3T3 mouse fibroblasts in 500 μl low-glucose DMEM (Sigma, USA) with 10% FBS (Sigma, USA) and 1% of penicillin/streptomycin (Sigma, USA) were added into insert placed wells and incubated at 37° C overnight. To assess the biological activity of FGF released from cryogel, the experimental set up was divided into 3 groups: PBS

(negative control), 50 ng/ml of FGF (positive control), and FGF released from the cryogel (day 3). Images were taken at 0 hrs and then every 2 hrs using EVOS™ FL Auto 2 Imaging System (Invitrogen, USA). After 24 hrs of incubation, cells were fixed with 4% formaldehyde and stained with DAPI for further analysis of cells-free surface area using free license Fiji software.

4.2.6 HUVEC proliferation assay for assessing VEGF biological activity

The proliferation of HUVEC cells was measured using Alamar Blue staining protocol (ThermoFisher Scientific, USA) according to the manufacturer's instructions. 10^4 HUVEC cells/well were seeded into a 96-well plate (TPP, Switzerland). After cells adhered to the wells, 10 ng/ml VEGF (Sigma, USA), cryogel released VEGF (day 3) and PBS were added. 10 µl of Alamar Blue reagent was added into wells, and after 4 hours of incubation, the absorbance at 570 nm was measured. Average values were taken from six samples of each measured group.

4.2.7 MTT Assay for assessing IL-10 biological activity

The biological activity of IL-10 was assessed by the proliferation of MC/9 cells. 5 x 10^3 of MC/9 cells were treated with 50 ng/ml IL-4 (Sigma, USA); 25 ng/ml IL-10 (Gibco, USA); 50 ng/ml IL-4 + 25 ng/ml IL-10; cryogel sample (Day 3), and cryogel sample + 50 ng/ml IL-4. Cells were incubated at 37° C for two days and followed by the addition of 10 µl of 3-(4,5-dimethylthiazol-2-yl)-2,5-diphenyl tetrazolium bromide (MTT solution) to each well. After 4-6 hrs incubation at 37° C, 100 µl of 10% SDS in 0.01M HCl was added to each well and the absorbance was measured at 570 nm (Varioskan Flash, Thermo Scientific, USA).

4.2.8 MTT Assay for assessing TGF-β biological activity

5 x 10^3 of NMuMG cells in the well were treated with: PBS, 2 ng/ml TGF-β (Gibco, USA), and cryogel sample TGF-β (Day 3). Cells were incubated at 37° C for 48 hours before proceeding with MTT assay. 10 μl MTT solution was added to each well and left at the incubator for 4-6 hrs. After incubation, 100 μl of isopropanol in 0.04M HCl was added to each well and the absorbance was measured at 570 nm (Varioskan Flash, Thermo Scientific, USA).

4.3 RESULTS

4.3.1 Growth Factors/Cytokines release kinetics from cryogel

To determine the effectiveness of cryogel as a drug delivery system, the rate of growth factors and cytokines release was evaluated over 10 days. Four groups containing different growth factors and cytokines (secreted factors) were prepared: 1 μg/ml, 0.3 μg/ml and 0.1 μg/ml of TGF-β and IL-10 or 10 μg/ml, 3 μg/ml and 1 μg/ml of VEGF and FGF. Loaded proteins should bind PEC-based cryogel via electrostatic interactions. Secreted factors loaded cryogels were incubated with 37° C with 10,000 U/ml of lysozyme [231] to mimic *in vivo* environment due to the ability of lysozyme to degrade CHI. Supernatants were collected at the specific days (1, 3, 5, 7 and 10) and the released concentration of loaded secreted factors was measured using ELISA. Figure 9 demonstrates that cryogel releases secreted factors in a controlled manner.

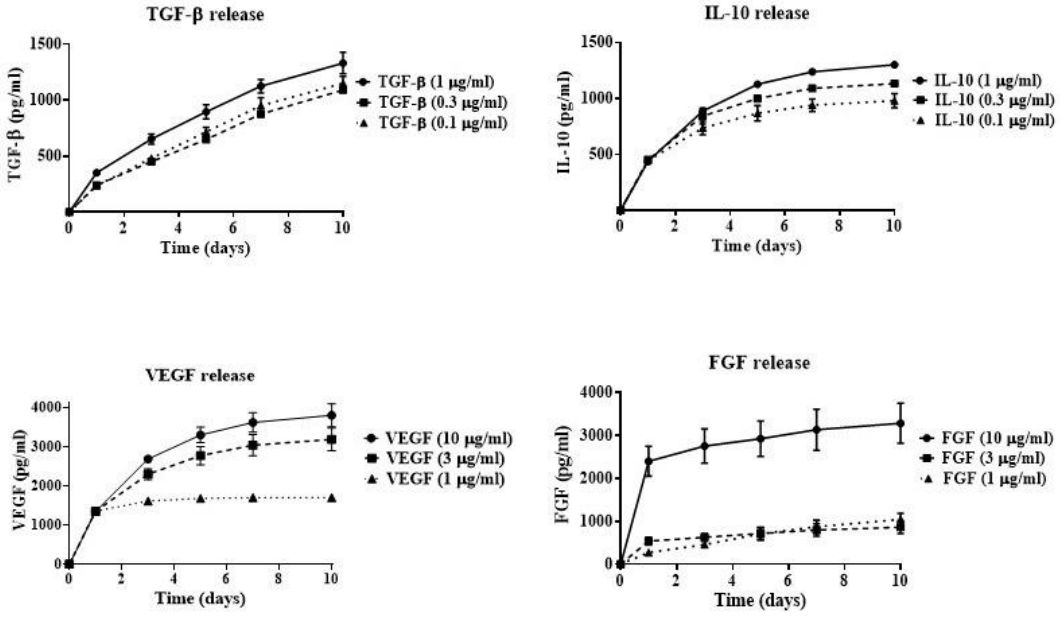

Figure 9. Release kinetics of secreted factors. Cumulative release is demonstrated, ELISA measurements were at 1, 3, 5, 7 and 10 days.

The cumulative release of TGF-β and IL-10 increases gradually reaching the highest release at 1 μg/ml. In contrast, VEGF and FGF loaded cryogels show similar results demonstrating the highest release at 10 μg/ml concentration and plateau after day 1 at low concentration (Figure 9). Obtained data demonstrate high loading efficiency and sustained release of loaded substances. Based on this the highest concentrations of secreted factors were used in subsequent experiments.

4.3.2 Assessing Biological activity of released secreted factors

The supernatants collected on day 3 were used to perform *in vitro* experiments on different cell models. For TGF-β, epithelial mouse mammary gland (NMuMG) cells were used due to the ability of TGF-β to suppress the proliferation of these cells. It was shown that TGF-β significantly inhibits the proliferation of NMuMG cells *in vitro* [232]. Our data also shows that TGF-β released from cryogel also inhibits the proliferation (34%) of NMuMG (Figure 10a) and thus biologically active. IL-10 biological activity was tested using MC/9 mast cells [233] because they proliferate when IL-10 and IL-4 are added *in vitro*. The proliferation of the MV/9 cells increases

by 68% for IL-4 and by 23% for IL-10 respectively (Figure 10b). The combination of both IL-10 and IL-4 increases MC/9 cell proliferation more than a two-fold (118%) and a similar increase in cell proliferation is demonstrated when cryogel released IL-10 is used (93%). Thus showing IL-10 sustains it biologically activity when released from cryogel.

HUVEC cells were used to test the biological activity of VEGF [234]. Released VEGF has the same effect on HUVEC cells as non-loaded VEGF (Figure 10c) demonstrating that VEGF released from cryogel is biologically active. A wound healing assay using NIH/3T3 cells was used to verify the activity of cryogel released FGF *in vitro*. NIH/3T3 fibroblasts proliferate when FGF is added [235]. The closure rate of the artificially made gap and surface area were calculated after overnight incubation of cells. Fibroblast proliferation under cryogel released FGF group demonstrates the

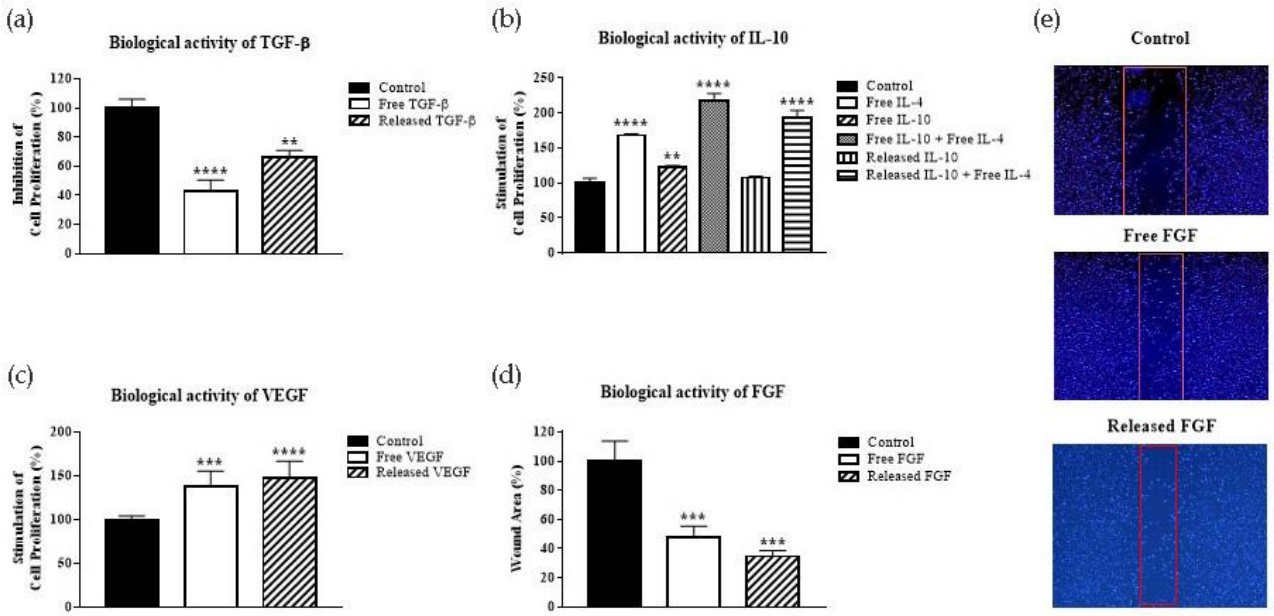

Figure 10. Biological activity experiments. (a) Inhibition of NMuMG proliferation by the cryogel released TGF-β, (b) Stimulation of MC/9 proliferation by the cryogel released IL-10, (c) Stimulation of HUVEC proliferation by the cryogel released VEGF, (d) Decrease in the wound area by the cryogel released FGF, (e) Wound areas are quantified in panel d. Data were analyzed using one-way ANOVA with Bonferroni's multiple comparisons test. $^{**}p < 0.01$, $^{***}p < 0.001$, $^{****}p < 0.0001$ compared with the control group.

same rate as the free FGF group. Wound closure was 53% higher for free FGF and

65% higher for released FGF in comparison to the control group (Figure 10d and e). It is important to note that the amount of released FGF was lower than in the positive group demonstrating that even the smaller amounts of the released growth factors/cytokines are enough to have a biological effect.

4.3.3 Effect on Wound Healing

This part of the research was done by Dr Shiro Jimi from Fukuoka University (Japan), materials and methods used are described in [27]. Novel PEC-based cryogels samples with protocols for loading secreted factors were shared with Dr Shiro to assess the efficacy of the developed strategy to induce wound regeneration *in vivo*.

The internal splint model established by Dr Shiro's group was used [236], the wound was located on the back of the mice. It is generally accepted that the inflammation stage occurs in the first 3 days and the proliferation stage is initiated after inflammation [237]. Therefore, the addition of growth factors and cytokines at days 0 and 3 were chosen as the most appropriate timing. Anti-inflammatory factors (TGF-β/ IL-10) should be added at day 0 and proliferation-inducing factors should be added on day 3. To determine whether cryogel loaded with secreted factors affect wound regeneration, the four groups of mice were established.

The first group was treated on days 0 and 3 with cryogel (Group with cryogel), the second group was treated on day 0 with cryogel containing TGF-β/ IL-10 and on day 3 with cryogel alone (Group with cryogel +TGF-β/IL-10). The third group was treated on day 0 with cryogel alone and on day 3 with the cryogel incorporated with VEGF/FGF (Group with cryogel + VEGF/FGF). The fourth group was treated on day 0 with cryogel containing TGF-β/IL-10 and on day 3 with cryogel containing VEGF/FGF on day 3 (Group with cryogel + GF/C). On day 3, before the addition of cryogel materials, wounds were cleared from previously applied cryogels. Obtained data show no statistically significant difference between the groups treated with

cryogel alone and groups containing only one pair of secreted factors only groups (2 and 3) (Figure 11). Group 4, where the sequential delivery of GF/C was made, the wound area is significantly reduced in comparison to all groups. It is important to note the treatment with factors alone without cryogel: TGF-β/IL-10 on day 0 and VEGF/FGF on day 3 didn't improve wound area closure (not included). Possibly, the proteolytic enzymes in the wound area degraded cryogel free GF/C factors. Obtained data shows that the most efficient wound healing is stimulated by group 4. To further assess the efficacy of sequential delivery cryogel loaded GF/C the mice were divided into three groups: control group (no treatment), cryogel alone group applied on days 0 and 3, and cryogel loaded with GF/C applied with TGF-β/IL-10 on day 0 and VEGF/FGF on day 3. Sample images of the wounds on day 10 are shown in Figure 12a. The dynamics of the healing presenting wound area decrease is demonstrated (Figure 12b). In the no treatment and cryogel alone groups, on day 10, wound closed by 35-40%, whereas the treatment group (cryogel+GF/C) wound closure by 87%. The sections of the wounds were also examined (Figure 12c).

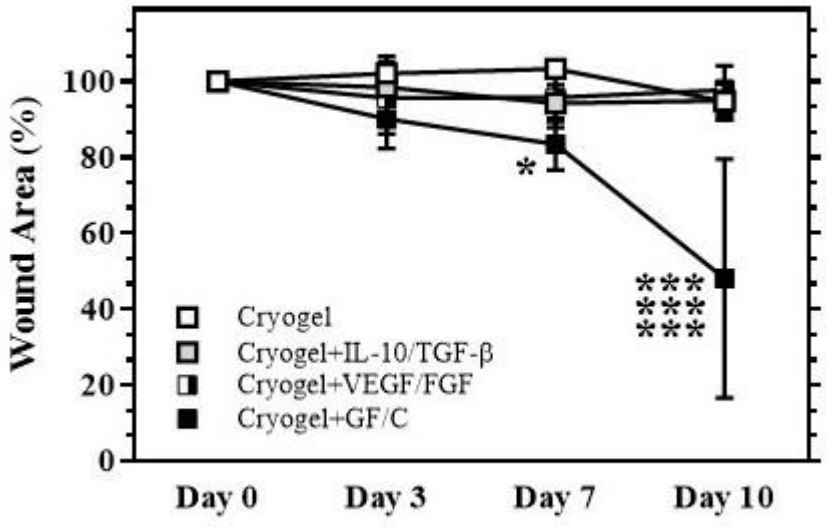

Figure 11. Wound healing after treatment with different cryogel groups: treated with cryogel alone, cryogel + IL-10/TGF-β, cryogel +VEGF/FGF and cryogel + all factors (GF/C). Wound area changes over time are shown (% vs. Day 0). Wound areas in the fourth group (cryogel + GF/C) significantly decreased on days 7 and 10 in comparison to the other groups. Values: mean ± SE. ***$p < 0.01$ compared to other groups, *$p < 0.05$ compared to cryogel alone group.

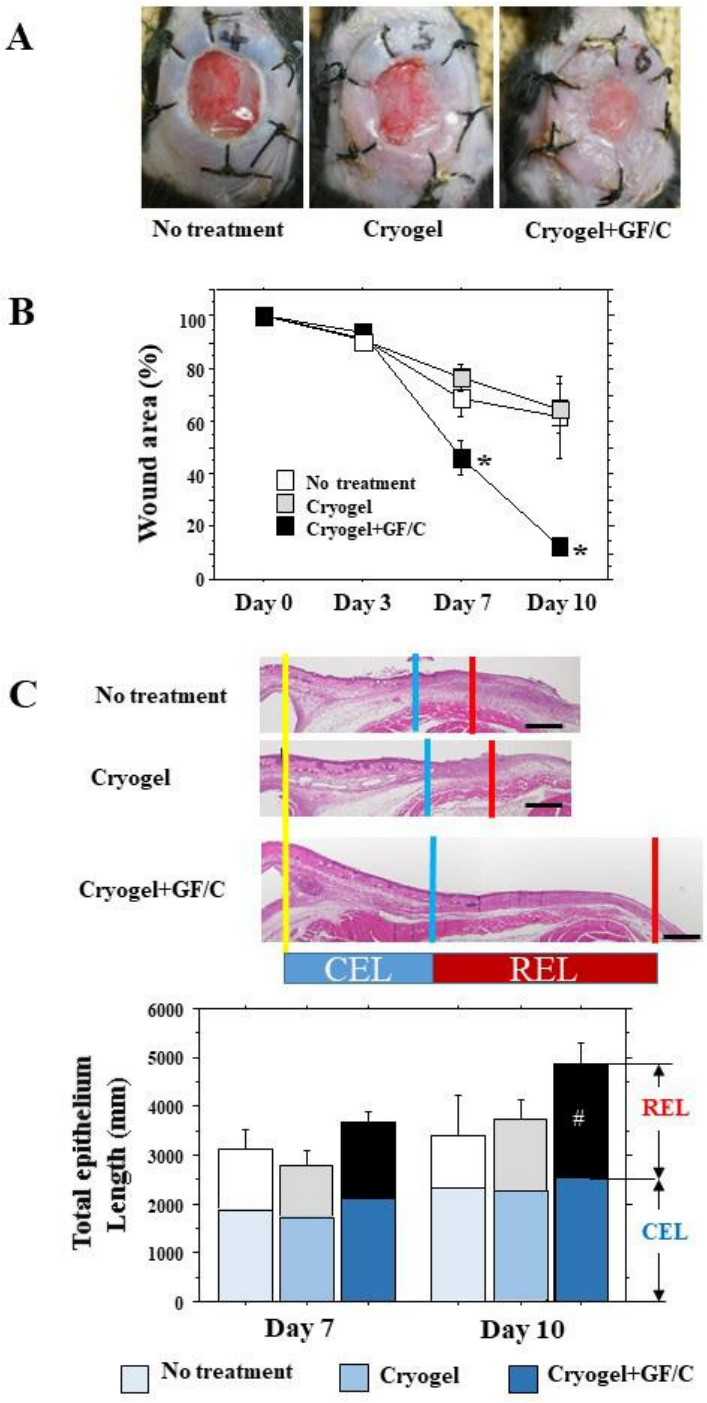

Figure 12. Wound healing and epithelial regeneration. (a) Sample images of wound closure on day 10. (b) Wound area (% vs. Day 0) over time. Wound areas in the cryogel+GF/C group significantly decreased on days 7 and 10 in comparison to others. (c) Wound epithelization. Epithelialization was evaluated as CEL and REL. Total epithelial length (CEL+REL) increased with time in all groups, with the same CEL among all groups. REL in cryogel+GF/C on day 10 was significantly longer in comparison to other groups. n=5. Bar=100 μm. Values: mean ± SE. *$p < 0.05$ compared to the no treatment group and group with cryogel alone, #$p < 0.05$ compared to the no treatment group.

A contractive length of the epidermis (CEL), regenerative length of the epidermis (REL), and total epithelial length (TEL) were also measured. On days 7 and 10, there

are no significant differences in CEL and TEL among the groups, however, REL on day 10, shows significant elongation in the cryogel+GF/C group in comparison to the secreted factors free groups.

4.3.4 Tissue granulation and collagenosis

The proliferative granulation tissues were present at every group, however, the thickness of granulated tissue was different among the groups. For the analysis, the edge of the growing epidermis was studied (Figure 13a). On day 10, the granulation thickness in cryogel alone and cryogel +GF/C groups was significantly greater in comparison to no treatment (Figure 13b, left panel). Collagenosis in the granulation

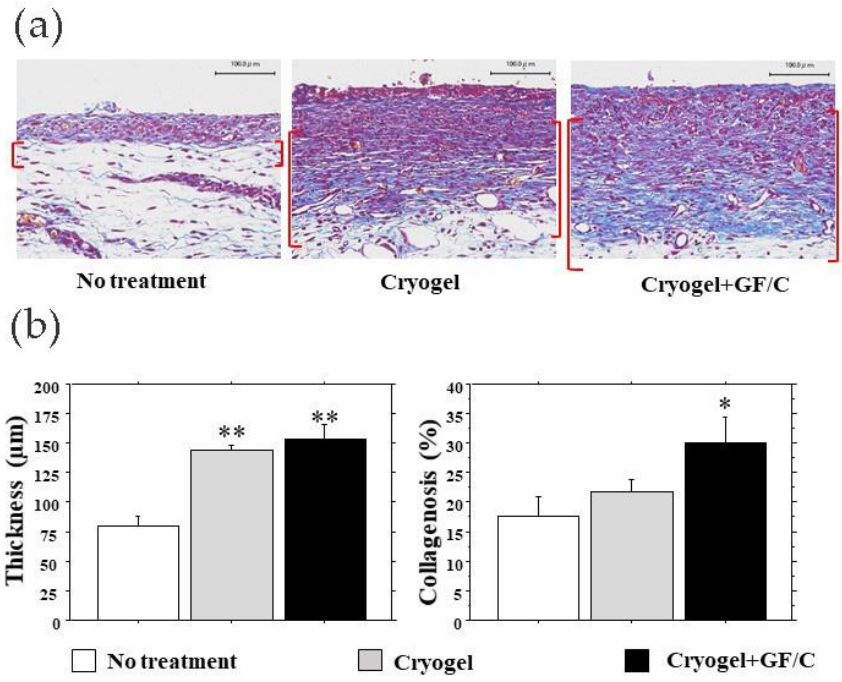

Figure 13. Granulation tissue and collagenosis. (a) Granulation tissue MT stained (blue). (b) Tissue thickness graph. Granulations in the groups with cryogel alone and cryogel+GF/C were significantly thicker in comparison to no treatment group. Collagenosis in the group with cryogel+GF/C progressed significantly as compared to the group with no treatment group. n=5. Bar=100 μm. Values: mean ± SE. *$p < 0.05$, **$p < 0.01$ compared to the no treatment group.

tissue was measured by MT staining (blue color) demonstrating a significant difference between cryogel + GF/C and no-treatment groups. Interestingly, no difference was found between no treatment and cryogel alone groups (Figure 13b, right panel).

Also, experiments on detecting neovascularization and blood flow measurement at the injured sites were conducted and published in [27].

4.4 DISCUSSION

Cells of the immune system and their secreted factors are an important part of tissue regeneration [238]. Neutrophils migrate into the injury site and produce ROS which further damages tissue [239]. Cellular debris is cleaned by migrated monocytes which also secrete various paracrine molecules and participate in the wound healing process [240]. Wound healing is the complex process that depends on growth factors, cytokines, cells and is the well-orchestrated process of tissue regeneration [240]. For healthy tissue regeneration, a fine balance between the local tissue environment and immune cells should be reached. There is a fine balance between the detrimental and beneficial effects of the cells of the immune system during inflammation [240]. Hyperinflammation at the site of the injury worsens tissue damage, leading to defective tissue repair [241]. Decreasing inflammation sometimes could be beneficial for accelerating tissue regeneration [242]. Here, a novel CHI containing PEC-based cryogel was used to modulate and enhance wound repair. The presence of CHI in cryogel gives to biomaterial water-holding and antimicrobial properties, it is biodegradable, which important for improving wound healing [243]. Secreted factors such as growth factors and cytokines are easily incorporated into cryogel due to positively and negatively charged residues, and more importantly, cryogel supports sustained release of bound factors [2]. Two cryogels containing two different bound secreted factors were used. Cryogel was incorporated with TGF-β and IL-10 because

they regulate response and suppress hyperinflammation VEGF and FGF were incorporated because they stimulate neovascularization, proliferation and tissue regeneration. All secreted factors show sustained release kinetics assuring a gradual increase of released factors. The released factors maintained their biological activity *in vitro*. TGF-β suppressed NMuMG cell proliferation, IL-10/IL-4 pair induced the proliferation of MC/9 cells, VEGF stimulated the proliferation of HUVEC cells and FGF stimulated proliferation of NIH/3T3 cells.

In vivo mice model showed cell infiltration with macrophages and neutrophils, but this was resolved during healing when tissue granulation was established. Cryogel was dissolved (biodegraded) on day 7 (last cryogel placed on day 3) which is beneficial for epithelization as mechanical removal could damage newly formed epithelial tissue and not degrading biomaterial could cause chronic inflammation, which should be avoided. It is important to note that the granulation tissue after cryogel+GF/C treatment has demonstrated positive myofibroblasts infiltration and CD31-positive neovascularization. Granulation gradually regresses during the normal healing process, it is formed at initial stages to fill the tissue at the site of injury [244]. Granulation tissue is required for the migrating cells to the wound site and modulated tissue regeneration [245]. The analysis was focused on granulation located at the edge of the growing epidermis, which could be implicated in the epidermal extension. CHI-based hydrogels have shown their efficacy for wound healing, however, the exact mechanisms are still elusive [246]. Groups of mice treated with cryogel independent of the GF/C presence developed granulation, whereas the cryogel free group does not. Interestingly, collagen synthesis significantly advanced only in cryogel+GF/C group. Cryogel itself caused granulation development, however, it wasn't enough to achieve tissue epithelialization. From this, we can conclude that secreted factors released from the cryogel significantly contributed to

the wound healing. It is important to note that neovascularization was also found to significantly increase in cryogel+GF/C group [27].

4.5 SUMMARY

To conclude, this study is the first to show the pathophysiological effect of cryogels on wound healing stimulation. Novel PEC-based cryogel acted not only as a drug delivery vehicle for secreted factors but as a scaffold for tissue cells, and thus accelerated the wound healing. The novel CHI/Hep containing PEC-based cryogel has shown its high biocompatibility properties, biodegradability after several days *in vivo*. These suggest that developed cryogel and cryogels themselves. It is obvious that developed cryogel and cryogels as s scaffold themselves may have the potential for practical use in wound healing applications and could be used in clinical practice in the future wound healing treatments in clinical practice in the future.

CONCLUSION AND FUTURE PERSPECTIVES

Today, along with the progress made in the use of stem cells, tissue engineering is becoming an important tool and research area, to reproduce the structure of tissues and help the same stem cells to become more effective. Scientists, pharmaceutical companies are developing a wide range of different biomaterials. They may have both a synthetic and a natural nature, with their advantages and disadvantages.

Extracellular matrix has a polymer base, it is very important to recreate its structure when developing biomaterial, as well as to give biodegradation property since it is assumed to be replaced by a natural matrix when creating any biomaterial. Depending on the tissue in which the material is implanted, the ability of the polymer to stimulate angiogenesis must be taken into account. The material should be biocompatible, not cytotoxic, or immunogenic. Based on these conditions, we can conclude that biomaterials made from the natural polymers are most appropriate.

There are a large number of biomaterials in various forms, such as gels, sponges, film and fiber, bioglasses, composites, and their possible variations. Each of them has its advantages and each of them is designed for use in the regeneration of certain tissues.

Work on the design of cryogel from natural components, such as chitosan and heparin, has been done in the current thesis. The resulting cryogels have porous structures with interconnected channels. A very important point is that this cryogel was created for the first time, it is very difficult to obtain cryogels with chitosan and heparin due to the immediate development of the polyelectrolyte complex.

During the experiments it was revealed that PVA inhibits the rate of polyelectrolyte formation, which in turn makes it possible to synthesize cryogel, nevertheless, the cryogel is still a polyelectrolyte, as was shown in the SEM images.

The presence of heparin is of great benefit since a large number of growth factors, cytokines and other molecules either have heparin-binding domains or interact with

heparin through electrostatic interactions. The presence of a polyelectrolyte complex enhances electrostatic interactions to load a wider range of proteins and molecules.

In the first experimental part, we have shown that the cryogel we developed is capable of loading BMP-2, as well as supporting osteogenic differentiation of rat bone marrow-derived mesenchymal stem cells in vitro. In addition to the main polymer components, we added hydroxyapatite to the cryogel formulation to improve its mechanical properties. Moreover, hydroxyapatite is part of the bone structure and is already a component of composite implants for bone regeneration. In this study, we showed that BMP-2 can be loaded without using any additional cross-linking agents, only by electrostatic interaction between the growth factor and cryogel.

Further, in a collaboration with Dr. Shiru from Fukuoka University (Japan), we evaluated our cryogel not only as a biomaterial but also as a delivery vehicle for growth factors and cytokines in wound healing model *in vivo*. The developed cryogel itself demonstrated its effectiveness in comparison with the control groups, and the cryogel loaded with growth factors and cytokines improved these results.

Sequential delivery of cytokines and growth factors stimulates wound healing, stimulates angiogenesis and epithelization, and our cryogel has shown its good biodegradability on wounds, which is an advantage for wound healing applications.

Further work, of course, will require more extensive and detailed experiments to evaluate the cryogel effectiveness for various injuries; fundamental questions remain about the effect of PVA on the formation of an electrolyte complex. Moreover, the safety of growth factors especially TGF-β should be clinically proven, its effect on priming cancer during the prolonged exposure. We believe that our published articles will allow other researchers to further study our developed biomaterial and introduce new designs and the use of cryogel for tissue regeneration applications.

REFERENCES

1. Sultankulov, B.; Berillo, D.; Sultankulova, K.; Tokay, T.; Saparov, A. Progress in the Development of Chitosan-Based Biomaterials for Tissue Engineering and Regenerative Medicine. *Biomolecules* **2019**, *9*, 470.
2. Sultankulov, B.; Berillo, D.; Kauanova, S.; Mikhalovsky, S.; Mikhalovska, L.; Saparov, A. Composite Cryogel with Polyelectrolyte Complexes for Growth Factor Delivery. *Pharmaceutics* **2019**, *11*, 650.
3. Oryan, A.; Alidadi, S.; Moshiri, A.; Maffulli, N. Bone regenerative medicine: classic options, novel strategies, and future directions. *J. Orthop. Surg. Res.* **2014**, *9*, 18.
4. Rodríguez-Vázquez, M.; Vega-Ruiz, B.; Ramos-Zúñiga, R.; Saldaña-Koppel, D.A.; Quiñones-Olvera, L.F. Chitosan and Its Potential Use as a Scaffold for Tissue Engineering in Regenerative Medicine. *Biomed Res. Int.* **2015**, *2015*, 1–15.
5. Hoven, V.P.; Tangpasuthadol, V.; Angkitpaiboon, Y.; Vallapa, N.; Kiatkamjornwong, S. Surface-charged chitosan: Preparation and protein adsorption. *Carbohydr. Polym.* **2007**, *68*, 44–53.
6. Saranya, N.; Moorthi, A.; Saravanan, S.; Devi, M.P.; Selvamurugan, N. Chitosan and its derivatives for gene delivery. *Int. J. Biol. Macromol.* **2011**, *48*, 234–238.
7. Venkatesan, J.; Anil, S.; Kim, S.K.; Shim, M.S. Chitosan as a vehicle for growth factor delivery: Various preparations and their applications in bone tissue regeneration. *Int. J. Biol. Macromol.* 2017, *104*, 1383–1397.
8. Raghavendra, G.M.; Varaprasad, K.; Jayaramudu, T. Biomaterials: Design, Development and Biomedical Applications. In *Nanotechnology Applications for Tissue Engineering*; Elsevier Inc., 2015; pp. 21–44 ISBN 9780323353038.
9. Hamman, J.H. Chitosan based polyelectrolyte complexes as potential carrier materials in drug delivery systems. *Mar. Drugs* **2010**, *8*, 1305–22.
10. Lankalapalli, S.; Kolapalli, V.R.M. Polyelectrolyte complexes: A review of their

applicability in drug delivery technology. *Indian J. Pharm. Sci.* 2009, *71*, 481–487.

11. Boddohi, S.; Moore, N.; Johnson, P.A.; Kipper, M.J. Polysaccharide-based polyelectrolyte complex nanoparticles from chitosan, heparin, and hyaluronan. *Biomacromolecules* **2009**, *10*, 1402–1409.
12. Tharanathan, R.N.; Kittur, F.S. Chitin — The Undisputed Biomolecule of Great Potential. *Crit. Rev. Food Sci. Nutr.* **2003**, *43*, 61–87.
13. Ghormade, V.; Pathan, E.K.; Deshpande, M.V. Can fungi compete with marine sources for chitosan production? *Int. J. Biol. Macromol.* **2017**, *104*, 1415–1421.
14. Grifoll-Romero, L.; Pascual, S.; Aragunde, H.; Biarnés, X.; Planas, A. Chitin Deacetylases: Structures, Specificities, and Biotech Applications. *Polymers (Basel).* **2018**, *10*, 352.
15. Ahsan, S.M.; Thomas, M.; Reddy, K.K.; Sooraparaju, S.G.; Asthana, A.; Bhatnagar, I. Chitosan as biomaterial in drug delivery and tissue engineering. *Int. J. Biol. Macromol.* **2018**, *110*, 97–109.
16. Alvarez, F.J. The Effect of chitin size, shape, source and purification method on immune recognition. *Molecules* **2014**, *19*, 4433–4451.
17. Balau, L.; Lisa, G.; Popa, M.; Tura, V.; Melnig, V. Physico-chemical properties of Chitosan films. *Open Chem.* **2004**, *2*, 638–647.
18. Fan, M.; Hu, Q.; Shen, K. Preparation and structure of chitosan soluble in wide pH range. *Carbohydr. Polym.* **2009**, *78*, 66–71.
19. Roberts, G.A.F. Solubility and Solution Behaviour of Chitin and Chitosan. In *Chitin Chemistry*; Macmillan Education UK: London, 1992; pp. 274–329.
20. Berillo, D.; Mattiasson, B.; Kirsebom, H. Cryogelation of chitosan using noble-metal ions: in situ formation of nanoparticles. *Biomacromolecules* **2014**, *15*, 2246–55.
21. Berillo, D.; Cundy, A. 3D-macroporous chitosan-based scaffolds with in situ formed Pd and Pt nanoparticles for nitrophenol reduction. *Carbohydr. Polym.*

2018, *192*, 166–175.

22. Berillo, D.; Elowsson, L.; Kirsebom, H. Oxidized Dextran as Crosslinker for Chitosan Cryogel Scaffolds and Formation of Polyelectrolyte Complexes between Chitosan and Gelatin. *Macromol. Biosci.* **2012**, *12*, 1090–1099.
23. Akilbekova, D.; Shaimerdenova, M.; Adilov, S.; Berillo, D. Biocompatible scaffolds based on natural polymers for regenerative medicine. *Int. J. Biol. Macromol.* **2018**, *114*, 324–333.
24. Lu, H.-T.; Lu, T.-W.; Chen, C.-H.; Lu, K.-Y.; Mi, F.-L. Development of nanocomposite scaffolds based on biomineralization of N,O-carboxymethyl chitosan/fucoidan conjugates for bone tissue engineering. *Int. J. Biol. Macromol.* **2018**, *120*, 2335–2345.
25. Nilsen-Nygaard, J.; Strand, S.; Vårum, K.; Draget, K.; Nordgård, C.; Nilsen-Nygaard, J.; Strand, S.P.; Vårum, K.M.; Draget, K.I.; Nordgård, C.T. Chitosan: Gels and Interfacial Properties. *Polymers (Basel).* **2015**, *7*, 552–579.
26. Badwan, A.; Rashid, I.; Omari, M.; Darras, F. Chitin and Chitosan as Direct Compression Excipients in Pharmaceutical Applications. *Mar. Drugs* **2015**, *13*, 1519–1547.
27. Jimi, S.; Jaguparov, A.; Nurkesh, A.; Sultankulov, B.; Saparov, A. Sequential Delivery of Cryogel Released Growth Factors Accelerates Wound Healing and Improves Tissue Regeneration. *Front. Bioeng. Biotechnol.* **2020**, *8*, 345.
28. Rousselle, P.; Montmasson, M.; Garnier, C. Extracellular matrix contribution to skin wound re-epithelialization. *Matrix Biol.* **2019**, *75–76*, 12–26.
29. Clark, R. Wound repair: Lessons for tissue engineering. In *Principles of tissue engineering*; Academic Press San Diego, 1997.
30. Abdelrahman, T.; Newton, H. Wound dressings: principles and practice. *Surg.* **2011**, *29*, 491–495.
31. Khan, M.A.; Mujahid, M. A review on recent advances in chitosan based

composite for hemostatic dressings. *Int. J. Biol. Macromol.* **2019**, *124*, 138–147.

32. Hu, Z.; Lu, S.; Cheng, Y.; Kong, S.; Li, S.; Li, C.; Yang, L. Investigation of the Effects of Molecular Parameters on the Hemostatic Properties of Chitosan. *Molecules* **2018**, *23*.
33. Yang, J.; Tian, F.; Wang, Z.; Wang, Q.; Zeng, Y.-J.; Chen, S.-Q. Effect of chitosan molecular weight and deacetylation degree on hemostasis. *J. Biomed. Mater. Res. Part B Appl. Biomater.* **2008**, *84B*, 131–137.
34. Guo, X.; Sun, T.; Zhong, R.; Ma, L.; You, C.; Tian, M.; Li, H.; Wang, C. Effects of Chitosan Oligosaccharides on Human Blood Components. *Front. Pharmacol.* **2018**, *9*, 1412.
35. Zhou, X.; Zhang, X.; Zhou, J.; Li, L. An investigation of chitosan and its derivatives on red blood cell agglutination. *RSC Adv.* **2017**, *7*, 12247–12254.
36. Klokkevold, P.R.; Fukayama, H.; Sung, E.C.; Bertolami, C.N. The effect of chitosan (poly-N-acetyl glucosamine) on lingual hemostasis in heparinized rabbits. *J. Oral Maxillofac. Surg.* **1999**, *57*, 49–52.
37. Hattori, H.; Ishihara, M. Changes in blood aggregation with differences in molecular weight and degree of deacetylation of chitosan. *Biomed. Mater.* **2015**, *10*, 015014.
38. Hu, Z.; Zhang, D.-Y.; Lu, S.-T.; Li, P.-W.; Li, S.-D. Chitosan-Based Composite Materials for Prospective Hemostatic Applications. *Mar. Drugs* **2018**, *16*.
39. Ueno, H.; Yamada, H.; Tanaka, I.; Kaba, N.; Matsuura, M.; Okumura, M.; Kadosawa, T.; Fujinaga, T. Accelerating effects of chitosan for healing at early phase of experimental open wound in dogs. *Biomaterials* **1999**, *20*, 1407–14.
40. Park, C.J.; Gabrielson, N.P.; Pack, D.W.; Jamison, R.D.; Wagoner Johnson, A.J. The effect of chitosan on the migration of neutrophil-like HL60 cells, mediated by IL-8. *Biomaterials* **2009**, *30*, 436–444.
41. Bueter, C.L.; Lee, C.K.; Rathinam, V.A.K.; Healy, G.J.; Taron, C.H.; Specht, C.A.;

Levitz, S.M. Chitosan but Not Chitin Activates the Inflammasome by a Mechanism Dependent upon Phagocytosis. *J. Biol. Chem.* **2011**, *286*, 35447–35455.

42. Bueter, C.L.; Lee, C.K.; Wang, J.P.; Ostroff, G.R.; Specht, C.A.; Levitz, S.M. Spectrum and Mechanisms of Inflammasome Activation by Chitosan. *J. Immunol.* **2014**, *192*, 5943–5951.
43. Gudmundsdottir, S.; Lieder, R.; Sigurjonsson, O.E.; Petersen, P.H. Chitosan leads to downregulation of YKL-40 and inflammasome activation in human macrophages. *J. Biomed. Mater. Res. Part A* **2015**, *103*, 2778–2785.
44. Fong, D.; Grégoire-Gélinas, P.; Cheng, A.P.; Mezheritsky, T.; Lavertu, M.; Sato, S.; Hoemann, C.D. Lysosomal rupture induced by structurally distinct chitosans either promotes a type 1 IFN response or activates the inflammasome in macrophages. *Biomaterials* **2017**, *129*, 127–138.
45. Vasconcelos, D.P.; de Torre-Minguela, C.; Gomez, A.I.; Águas, A.P.; Barbosa, M.A.; Pelegrín, P.; Barbosa, J.N. 3D chitosan scaffolds impair NLRP3 inflammasome response in macrophages. *Acta Biomater.* **2019**.
46. Baxter, R.M.; Dai, T.; Kimball, J.; Wang, E.; Hamblin, M.R.; Wiesmann, W.P.; McCarthy, S.J.; Baker, S.M. Chitosan dressing promotes healing in third degree burns in mice: gene expression analysis shows biphasic effects for rapid tissue regeneration and decreased fibrotic signaling. *J. Biomed. Mater. Res. A* **2013**, *101*, 340–8.
47. Tsai, C.-W.; Chiang, I.-N.; Wang, J.-H.; Young, T.-H. Chitosan delaying human fibroblast senescence through downregulation of TGF-β signaling pathway. *Artif. Cells, Nanomedicine, Biotechnol.* **2017**, *46*, 1–12.
48. Howling, G.I.; Dettmar, P.W.; Goddard, P.A.; Hampson, F.C.; Dornish, M.; Wood, E.J. The effect of chitin and chitosan on the proliferation of human skin fibroblasts and keratinocytes in vitro. *Biomaterials* **2001**, *22*, 2959–66.
49. Hamilton, V.; Yuan, Y.; Rigney, D.A.; Puckett, A.D.; Ong, J.L.; Yang, Y.; Elder,

S.H.; Bumgardner, J.D. Characterization of chitosan films and effects on fibroblast cell attachment and proliferation. *J. Mater. Sci. Mater. Med.* **2006**, *17*, 1373–1381.

50. Croisier, F.; Jérôme, C. Chitosan-based biomaterials for tissue engineering. *Eur. Polym. J.* **2013**, *49*, 780–792.
51. Song, R.; Zheng, J.; Liu, Y.; Tan, Y.; Yang, Z.; Song, X.; Yang, S.; Fan, R.; Zhang, Y.; Wang, Y. A natural cordycepin/chitosan complex hydrogel with outstanding self-healable and wound healing properties. *Int. J. Biol. Macromol.* **2019**, *134*, 91–99.
52. Aubert-Viard, F.; Mogrovejo-Valdivia, A.; Tabary, N.; Maton, M.; Chai, F.; Neut, C.; Martel, B.; Blanchemain, N. Evaluation of antibacterial textile covered by layer-by-layer coating and loaded with chlorhexidine for wound dressing application. *Mater. Sci. Eng. C* **2019**, *100*, 554–563.
53. Alves, P.; Santos, M.; Mendes, S.; P. Miguel, S.; D. de Sá, K.; S. D. Cabral, C.; J. Correia, I.; Ferreira, P.; Alves, P.; Santos, M.; et al. Photocrosslinkable Nanofibrous Asymmetric Membrane Designed for Wound Dressing. *Polymers (Basel).* **2019**, *11*, 653.
54. Shah, A.; Ali Buabeid, M.; Arafa, E.-S.A.; Hussain, I.; Li, L.; Murtaza, G. The wound healing and antibacterial potential of triple-component nanocomposite (chitosan-silver-sericin) films loaded with moxifloxacin. *Int. J. Pharm.* **2019**, *564*, 22–38.
55. Lin, C.-W.; Chen, Y.-K.; Lu, M.; Lou, K.-L.; Yu, J. Photo-Crosslinked Keratin/Chitosan Membranes as Potential Wound Dressing Materials. *Polymers (Basel).* **2018**, *10*, 987.
56. Sharma, S.; Swetha, K.L.; Roy, A. Chitosan-Chondroitin sulfate based polyelectrolyte complex for effective management of chronic wounds. *Int. J. Biol. Macromol.* **2019**, *132*, 97–108.

57. Karimi Dehkordi, N.; Minaiyan, M.; Talebi, A.; Akbari, V.; Taheri, A. Nanocrystalline cellulose–hyaluronic acid composite enriched with GM-CSF loaded chitosan nanoparticles for enhanced wound healing. *Biomed. Mater.* **2019**, *14*, 035003.

58. Koukaras, E.N.; Papadimitriou, S.A.; Bikiaris, D.N.; Froudakis, G.E. Insight on the Formation of Chitosan Nanoparticles through Ionotropic Gelation with Tripolyphosphate. *Mol. Pharm.* **2012**, *9*, 2856–2862.

59. Tanha, S.; Rafiee-Tehrani, M.; Abdollahi, M.; Vakilian, S.; Esmaili, Z.; Naraghi, Z.S.; Seyedjafari, E.; Javar, H.A. G-CSF loaded nanofiber/nanoparticle composite coated with collagen promotes wound healing *in vivo*. *J. Biomed. Mater. Res. Part A* **2017**, *105*, 2830–2842.

60. Chen, X.; Zhang, M.; Chen, S.; Wang, X.; Tian, Z.; Chen, Y.; Xu, P.; Zhang, L.; Zhang, L.; Zhang, L. Peptide-Modified Chitosan Hydrogels Accelerate Skin Wound Healing by Promoting Fibroblast Proliferation, Migration, and Secretion. *Cell Transplant.* **2017**, *26*, 1331–1340.

61. Chen, X.; Fu, W.; Cao, X.; Jiang, H.; Che, X.; Xu, X.; Ma, B.; Zhang, J. Peptide SIKVAV-modified chitosan hydrogels promote skin wound healing by accelerating angiogenesis and regulating cytokine secretion. *Am. J. Transl. Res.* **2018**, *10*, 4258–4268.

62. Yu, Y.; Chen, R.; Sun, Y.; Pan, Y.; Tang, W.; Zhang, S.; Cao, L.; Yuan, Y.; Wang, J.; Liu, C. Manipulation of VEGF-induced angiogenesis by 2-N, 6-O-sulfated chitosan. *Acta Biomater.* **2018**, *71*, 510–521.

63. Wang, C.; Yu, Y.; Chen, H.; Zhang, S.; Wang, J.; Liu, C. Construction of cytokine reservoirs based on sulfated chitosan hydrogels for the capturing of VEGF *in situ*. *J. Mater. Chem. B* **2019**, *7*, 1882–1892.

64. Titorencu, I.; Albu, M.; Nemecz, M.; Jinga, V. Natural Polymer-Cell Bioconstructs for Bone Tissue Engineering. *Curr. Stem Cell Res. Ther.* **2016**, *12*,

165–174.

65. Saravanan, S.; Leena, R.S.; Selvamurugan, N. Chitosan based biocomposite scaffolds for bone tissue engineering. *Int. J. Biol. Macromol.* **2016**, *93*, 1354–1365.
66. Deepthi, S.; Venkatesan, J.; Kim, S.-K.; Bumgardner, J.D.; Jayakumar, R. An overview of chitin or chitosan/nano ceramic composite scaffolds for bone tissue engineering. *Int. J. Biol. Macromol.* **2016**, *93*, 1338–1353.
67. He, L.-H.; Yao, L.; Xue, R.; Sun, J.; Song, R. In-situ mineralization of chitosan/calcium phosphate composite and the effect of solvent on the structure. *Front. Mater. Sci.* **2011**, *5*, 282–292.
68. Tuzlakoglu, K.; Reis, R.L. Formation of bone-like apatite layer on chitosan fiber mesh scaffolds by a biomimetic spraying process. *J. Mater. Sci. Mater. Med.* **2007**, *18*, 1279–1286.
69. Leonor, I.B.; Baran, E.T.; Kawashita, M.; Reis, R.L.; Kokubo, T.; Nakamura, T. Growth of a bonelike apatite on chitosan microparticles after a calcium silicate treatment. *Acta Biomater.* **2008**, *4*, 1349–1359.
70. Elkholy, S.; Yahia, S.; Awad, M.; Elmessiery, M. In vivo evaluation of β-CS/n-HA with different physical properties as a new bone graft material. *Clin. Implant Dent. Relat. Res.* **2018**, *20*, 416–423.
71. Gaihre, B.; Jayasuriya, A.C. Comparative investigation of porous nano-hydroxyapaptite/chitosan, nano-zirconia/chitosan and novel nano-calcium zirconate/chitosan composite scaffolds for their potential applications in bone regeneration. *Mater. Sci. Eng. C* **2018**, *91*, 330–339.
72. Koç Demir, A.; Elçin, A.E.; Elçin, Y.M. Strontium-modified chitosan/montmorillonite composites as bone tissue engineering scaffold. *Mater. Sci. Eng. C* **2018**, *89*, 8–14.
73. Georgopoulou, A.; Kaliva, M.; Vamvakaki, M.; Chatzinikolaidou, M. Osteogenic Potential of Pre-Osteoblastic Cells on a Chitosan-graft-

Polycaprolactone Copolymer. *Materials (Basel).* **2018**, *11*, 490.

74. Habibovic, P.; Barralet, J.E. Bioinorganics and biomaterials: Bone repair. *Acta Biomater.* 2011, *7*, 3013–3026.

75. Singh, B.N.; Veeresh, V.; Mallick, S.P.; Jain, Y.; Sinha, S.; Rastogi, A.; Srivastava, P. Design and evaluation of chitosan/chondroitin sulfate/nano-bioglass based composite scaffold for bone tissue engineering. *Int. J. Biol. Macromol.* **2019**, *133*, 817–830.

76. Georgopoulou, A.; Papadogiannis, F.; Batsali, A.; Marakis, J.; Alpantaki, K.; Eliopoulos, A.G.; Pontikoglou, C.; Chatzinikolaidou, M. Chitosan/gelatin scaffolds support bone regeneration. *J. Mater. Sci. Mater. Med.* **2018**, *29*, 59.

77. Lu, H.-T.; Lu, T.-W.; Chen, C.-H.; Mi, F.-L. Development of genipin-crosslinked and fucoidan-adsorbed nano-hydroxyapatite/hydroxypropyl chitosan composite scaffolds for bone tissue engineering. *Int. J. Biol. Macromol.* **2019**, *128*, 973–984.

78. Keller, L.; Regiel-Futyra, A.; Gimeno, M.; Eap, S.; Mendoza, G.; Andreu, V.; Wagner, Q.; Kyzioł, A.; Sebastian, V.; Stochel, G.; et al. Chitosan-based nanocomposites for the repair of bone defects. *Nanomedicine Nanotechnology, Biol. Med.* **2017**, *13*, 2231–2240.

79. Nguyen, T.H.M.; Abueva, C.; Ho, H. Van; Lee, S.-Y.; Lee, B.-T. In vitro and in vivo acute response towards injectable thermosensitive chitosan/TEMPO-oxidized cellulose nanofiber hydrogel. *Carbohydr. Polym.* **2018**, *180*, 246–255.

80. Zhang, L.; Wu, K.; Song, W.; Xu, H.; An, R.; Zhao, L.; Liu, B.; Zhang, Y. Chitosan/siCkip-1 biofunctionalized titanium implant for improved osseointegration in the osteoporotic condition. *Sci. Rep.* **2015**, *5*, 10860.

81. Dwivedi, P.; Narvi, S.S.; Tewari, R.P. Application of polymer nanocomposites in the nanomedicine landscape: envisaging strategies to combat implant associated infections. *J. Appl. Biomater. Funct. Mater.* **2013**, *11*, 129–142.

82. Kumar, A.M.; Suresh, B.; Das, S.; Obot, I.B.; Adesina, A.Y.; Ramakrishna, S. Promising bio-composites of polypyrrole and chitosan: Surface protective and in vitro biocompatibility performance on 316L SS implants. *Carbohydr. Polym.* **2017**, *173*, 121–130.

83. Liu, J.; Sun, L.; Xu, W.; Wang, Q.; Yu, S.; Sun, J. Current advances and future perspectives of 3D printing natural-derived biopolymers. *Carbohydr. Polym.* **2019**, *207*, 297–316.

84. Demirtaş, T.T.; Irmak, G.; Gümüşderelioğlu, M. A bioprintable form of chitosan hydrogel for bone tissue engineering. *Biofabrication* **2017**, *9*, 035003.

85. Liao, I.-C.; Moutos, F.T.; Estes, B.T.; Zhao, X.; Guilak, F. Composite Three-Dimensional Woven Scaffolds with Interpenetrating Network Hydrogels to Create Functional Synthetic Articular Cartilage. *Adv. Funct. Mater.* **2013**, *23*, 5833–5839.

86. Nettles, D.L.; Elder, S.H.; Gilbert, J.A. Potential Use of Chitosan as a Cell Scaffold Material for Cartilage Tissue Engineering. *Tissue Eng.* **2002**, *8*, 1009–1016.

87. Freedman, B.R.; Mooney, D.J. Biomaterials to Mimic and Heal Connective Tissues. *Adv. Mater.* **2019**, *31*, 1806695.

88. Jin, R.; Moreira Teixeira, L.S.; Dijkstra, P.J.; Karperien, M.; van Blitterswijk, C.A.; Zhong, Z.Y.; Feijen, J. Injectable chitosan-based hydrogels for cartilage tissue engineering. *Biomaterials* **2009**, *30*, 2544–2551.

89. Liu, M.; Zeng, X.; Ma, C.; Yi, H.; Ali, Z.; Mou, X.; Li, S.; Deng, Y.; He, N. Injectable hydrogels for cartilage and bone tissue engineering. *Bone Res.* **2017**, *5*, 17014.

90. Huang, H.; Zhang, X.; Hu, X.; Dai, L.; Zhu, J.; Man, Z.; Chen, H.; Zhou, C.; Ao, Y. Directing chondrogenic differentiation of mesenchymal stem cells with a solid-supported chitosan thermogel for cartilage tissue engineering. *Biomed.*

Mater. **2014**, *9*, 035008.

91. Kuo, C.-Y.; Chen, C.-H.; Hsiao, C.-Y.; Chen, J.-P. Incorporation of chitosan in biomimetic gelatin/chondroitin-6-sulfate/hyaluronan cryogel for cartilage tissue engineering. *Carbohydr. Polym.* **2015**, *117*, 722–730.
92. VandeVord, P.J.; Matthew, H.W.T.; DeSilva, S.P.; Mayton, L.; Wu, B.; Wooley, P.H. Evaluation of the biocompatibility of a chitosan scaffold in mice. *J. Biomed. Mater. Res.* **2002**, *59*, 585–90.
93. Choi, B.; Kim, S.; Lin, B.; Wu, B.M.; Lee, M. Cartilaginous Extracellular Matrix-Modified Chitosan Hydrogels for Cartilage Tissue Engineering. *ACS Appl. Mater. Interfaces* **2014**, *6*, 20110–20121.
94. Oprenyeszk, F.; Sanchez, C.; Dubuc, J.-E.; Maquet, V.; Henrist, C.; Compère, P.; Henrotin, Y. Chitosan enriched three-dimensional matrix reduces inflammatory and catabolic mediators production by human chondrocytes. *PLoS One* **2015**, *10*, e0128362.
95. Kong, Y.; Zhang, Y.; Zhao, X.; Wang, G.; Liu, Q. Carboxymethyl-chitosan attenuates inducible nitric oxide synthase and promotes interleukin-10 production in rat chondrocytes. *Exp. Ther. Med.* **2017**, *14*, 5641–5646.
96. Huang, S.; Song, X.; Li, T.; Xiao, J.; Chen, Y.; Gong, X.; Zeng, W.; Yang, L.; Chen, C. Pellet coculture of osteoarthritic chondrocytes and infrapatellar fat pad-derived mesenchymal stem cells with chitosan/hyaluronic acid nanoparticles promotes chondrogenic differentiation. *Stem Cell Res. Ther.* **2017**, *8*, 264.
97. Ye, K.; Felimban, R.; Traianedes, K.; Moulton, S.E.; Wallace, G.G.; Chung, J.; Quigley, A.; Choong, P.F.M.; Myers, D.E. Chondrogenesis of infrapatellar fat pad derived adipose stem cells in 3D printed chitosan scaffold. *PLoS One* **2014**, *9*, e99410.
98. Sionkowska, A.; Wisniewski, M.; Skopinska, J.; Kennedy, C.J.; Wess, T.J. Molecular interactions in collagen and chitosan blends. *Biomaterials* **2004**, *25*,

795–801.

99. Haaparanta, A.-M.; Järvinen, E.; Cengiz, I.F.; Ellä, V.; Kokkonen, H.T.; Kiviranta, I.; Kellomäki, M. Preparation and characterization of collagen/PLA, chitosan/PLA, and collagen/chitosan/PLA hybrid scaffolds for cartilage tissue engineering. *J. Mater. Sci. Mater. Med.* **2014**, *25*, 1129–1136.
100. Su, J.-Y.; Chen, S.-H.; Chen, Y.-P.; Chen, W.-C. Evaluation of Magnetic Nanoparticle-Labeled Chondrocytes Cultivated on a Type II Collagen-Chitosan/Poly(Lactic-co-Glycolic) Acid Biphasic Scaffold. *Int. J. Mol. Sci.* **2017**, *18*.
101. Bhardwaj, N.; Nguyen, Q.T.; Chen, A.C.; Kaplan, D.L.; Sah, R.L.; Kundu, S.C. Potential of 3-D tissue constructs engineered from bovine chondrocytes/silk fibroin-chitosan for in vitro cartilage tissue engineering. *Biomaterials* **2011**, *32*, 5773–81.
102. Liu, J.; Fang, Q.; Yu, X.; Wan, Y.; Xiao, B. Chitosan-Based Nanofibrous Membrane Unit with Gradient Compositional and Structural Features for Mimicking Calcified Layer in Osteochondral Matrix. *Int. J. Mol. Sci.* **2018**, *19*.
103. Noriega, S.E.; Hasanova, G.I.; Schneider, M.J.; Larsen, G.F.; Subramanian, A. Effect of fiber diameter on the spreading, proliferation and differentiation of chondrocytes on electrospun chitosan matrices. *Cells. Tissues. Organs* **2012**, *195*, 207–21.
104. Bhat, S.; Tripathi, A.; Kumar, A. Supermacroprous chitosan–agarose–gelatin cryogels: in vitro characterization and in vivo assessment for cartilage tissue engineering. *J. R. Soc. Interface* **2011**, *8*, 540.
105. Gupta, A.; Bhat, S.; Jagdale, P.R.; Chaudhari, B.P.; Lidgren, L.; Gupta, K.C.; Kumar, A. Evaluation of three-dimensional chitosan-agarose-gelatin cryogel scaffold for the repair of subchondral cartilage defects: an in vivo study in a rabbit model. *Tissue Eng. Part A* **2014**, *20*, 3101–11.

106. Lu, T.-J.; Chiu, F.-Y.; Chiu, H.-Y.; Chang, M.-C.; Hung, S.-C. Chondrogenic Differentiation of Mesenchymal Stem Cells in Three-Dimensional Chitosan Film Culture. *Cell Transplant.* **2017**, *26*, 417–427.

107. Vårum, K.M.; Holme, H.K.; Izume, M.; Stokke, B.T.; Smidsrød, O. Determination of enzymatic hydrolysis specificity of partially N-acetylated chitosans. *Biochim. Biophys. Acta* **1996**, *1291*, 5–15.

108. Rathore, A.S.; Gupta, R.D. Chitinases from Bacteria to Human: Properties, Applications, and Future Perspectives. *Enzyme Res.* **2015**, *2015*, 791907.

109. Sogias, I.A.; Williams, A.C.; Khutoryanskiy, V. V. Why is Chitosan Mucoadhesive? *Biomacromolecules* **2008**, *9*, 1837–1842.

110. Casettari, L.; Illum, L. Chitosan in nasal delivery systems for therapeutic drugs. *J. Control. Release* **2014**, *190*, 189–200.

111. Irimia, T.; Dinu-Pîrvu, C.-E.; Ghica, M.V.; Lupuleasa, D.; Muntean, D.-L.; Udeanu, D.I.; Popa, L. Chitosan-Based In Situ Gels for Ocular Delivery of Therapeutics: A State-of-the-Art Review. *Mar. Drugs* **2018**, *16*.

112. Batista, P.; Castro, P.; Madureira, A.R.; Sarmento, B.; Pintado, M. Development and Characterization of Chitosan Microparticles-in-Films for Buccal Delivery of Bioactive Peptides. *Pharmaceuticals (Basel).* **2019**, *12*.

113. Ortiz, M.; Jornada, D.S.; Pohlmann, A.R.; Guterres, S.S. Development of Novel Chitosan Microcapsules for Pulmonary Delivery of Dapsone: Characterization, Aerosol Performance, and In Vivo Toxicity Evaluation. *AAPS PharmSciTech* **2015**, *16*, 1033–40.

114. Baranwal, A.; Kumar, A.; Priyadharshini, A.; Oggu, G.S.; Bhatnagar, I.; Srivastava, A.; Chandra, P. Chitosan: An undisputed bio-fabrication material for tissue engineering and bio-sensing applications. *Int. J. Biol. Macromol.* **2018**, *110*, 110–123.

115. Ahmed, S.; Annu; Ali, A.; Sheikh, J. A review on chitosan centred scaffolds and

their applications in tissue engineering. *Int. J. Biol. Macromol.* **2018**, *116*, 849–862.

116. Xiangyang, X.; Ling, L.; Jianping, Z.; Shiyue, L.; Jie, Y.; Xiaojin, Y.; Jinsheng, R. Preparation and characterization of N-succinyl-N′-octyl chitosan micelles as doxorubicin carriers for effective anti-tumor activity. *Colloids Surfaces B Biointerfaces* **2007**, *55*, 222–228.
117. Mohammed, M.A.; Syeda, J.T.M.; Wasan, K.M.; Wasan, E.K. An Overview of Chitosan Nanoparticles and Its Application in Non-Parenteral Drug Delivery. *Pharmaceutics* **2017**, *9*.
118. Chen, K.-Y.; Zeng, S.-Y. Fabrication of Quaternized Chitosan Nanoparticles Using Tripolyphosphate/Genipin Dual Cross-Linkers as a Protein Delivery System. *Polymers (Basel).* **2018**, *10*.
119. Divya, K.; Jisha, M.S. Chitosan nanoparticles preparation and applications. *Environ. Chem. Lett.* **2018**, *16*, 101–112.
120. Özbaş-Turan, S.; Akbuğa, J.; Aral, C. Controlled Release of Interleukin-2 from Chitosan Microspheres. *J. Pharm. Sci.* **2002**, *91*, 1245–1251.
121. Samorezov, J.E.; Alsberg, E. Spatial regulation of controlled bioactive factor delivery for bone tissue engineering. *Adv. Drug Deliv. Rev.* **2015**, *84*, 45–67.
122. Lin, C.; Romero, R.; Sorokina, L. V; Ballinger, K.R.; Place, L.W.; Kipper, M.J.; Khetani, S.R. A polyelectrolyte multilayer platform for investigating growth factor delivery modes in human liver cultures. *J. Biomed. Mater. Res. A* **2018**, *106*, 971–984.
123. Tan, Q.; Tang, H.; Hu, J.; Hu, Y.; Zhou, X.; Tao, Y.; Wu, Z. Controlled release of chitosan/heparin nanoparticle-delivered VEGF enhances regeneration of decellularized tissue-engineered scaffolds. *Int. J. Nanomedicine* **2011**, *6*, 929–42.
124. Liang, Y.; Kiick, K.L. Heparin-functionalized polymeric biomaterials in tissue engineering and drug delivery applications. *Acta Biomater.* **2014**, *10*, 1588–600.
125. Mansurov, N.; Chen, W.C.W.; Awada, H.; Huard, J.; Wang, Y.; Saparov, A. A

controlled release system for simultaneous delivery of three human perivascular stem cell-derived factors for tissue repair and regeneration. *J. Tissue Eng. Regen. Med.* **2018**, *12*, e1164–e1172.

126. Pilipenko, I.; Korzhikov-Vlakh, V.; Sharoyko, V.; Zhang, N.; Schäfer-Korting, M.; Rühl, E.; Zoschke, C.; Tennikova, T. pH-Sensitive Chitosan–Heparin Nanoparticles for Effective Delivery of Genetic Drugs into Epithelial Cells. *Pharmaceutics* **2019**, *11*, 317.
127. Zeng, K.; Groth, T.; Zhang, K. Recent Advances in Artificially Sulfated Polysaccharides for Applications in Cell Growth and Differentiation, Drug Delivery, and Tissue Engineering. *ChemBioChem* **2019**, *20*, 737–746.
128. Zhong, Z.; Li, P.; Xing, R.; Liu, S. Antimicrobial activity of hydroxylbenzenesulfonailides derivatives of chitosan, chitosan sulfates and carboxymethyl chitosan. *Int. J. Biol. Macromol.* **2009**, *45*, 163–168.
129. Ho, Y.-C.; Wu, S.-J.; Mi, F.-L.; Chiu, Y.-L.; Yu, S.-H.; Panda, N.; Sung, H.-W. Thiol-Modified Chitosan Sulfate Nanoparticles for Protection and Release of Basic Fibroblast Growth Factor. *Bioconjug. Chem.* **2010**, *21*, 28–38.
130. Peschel, D.; Zhang, K.; Fischer, S.; Groth, T. Modulation of osteogenic activity of BMP-2 by cellulose and chitosan derivatives. *Acta Biomater.* **2012**, *8*, 183–193.
131. Weltrowski, A.; da Silva Almeida, M.-L.; Peschel, D.; Zhang, K.; Fischer, S.; Groth, T. Mitogenic Activity of Sulfated Chitosan and Cellulose Derivatives is Related to Protection of FGF-2 from Proteolytic Cleavage. *Macromol. Biosci.* **2012**, *12*, 740–750.
132. Farrugia, B.L.; Mi, Y.; Kim, H.N.; Whitelock, J.M.; Baker, S.M.; Wiesmann, W.P.; Li, Z.; Maitz, P.; Lord, M.S. Chitosan-Based Heparan Sulfate Mimetics Promote Epidermal Formation in a Human Organotypic Skin Model. *Adv. Funct. Mater.* **2018**, *28*, 1802818.
133. Mumper, R.; Wang, J.; Claspell, J.; Rolland, A. Novel polymeric condensing

carriers for gene delivery. *Proc. Control. Release Soc.* **1995**, *22*, 178–179.

134. Santos-Carballal, B.; Fernández Fernández, E.; Goycoolea, F.; Santos-Carballal, B.; Fernández Fernández, E.; Goycoolea, F.M. Chitosan in Non-Viral Gene Delivery: Role of Structure, Characterization Methods, and Insights in Cancer and Rare Diseases Therapies. *Polymers (Basel).* **2018**, *10*, 444.
135. Vauthier, C.; Zandanel, C.; Ramon, A.L. Chitosan-based nanoparticles for in vivo delivery of interfering agents including siRNA. *Curr. Opin. Colloid Interface Sci.* **2013**, *18*, 406–418.
136. Cryan, S.-A.; McKiernan, P.; Cunningham, C.M.; Greene, C. Targeting miRNA-based medicines to cystic fibrosis airway epithelial cells using nanotechnology. *Int. J. Nanomedicine* **2013**, *8*, 3907.
137. Ban, E.; Kwon, T.-H.; Kim, A. Delivery of therapeutic miRNA using polymer-based formulation. *Drug Deliv. Transl. Res.* **2019**.
138. Csaba, N.; Köping-Höggård, M.; Alonso, M.J. Ionically crosslinked chitosan/tripolyphosphate nanoparticles for oligonucleotide and plasmid DNA delivery. *Int. J. Pharm.* **2009**, *382*, 205–214.
139. Csaba, N.; Köping-Höggård, M.; Fernandez-Megia, E.; Novoa-Carballal, R.; Riguera, R.; Alonso, M.J. Ionically crosslinked chitosan nanoparticles as gene delivery systems: effect of PEGylation degree on in vitro and in vivo gene transfer. *J. Biomed. Nanotechnol.* **2009**, *5*, 162–71.
140. Mao, H.Q.; Roy, K.; Troung-Le, V.L.; Janes, K.A.; Lin, K.Y.; Wang, Y.; August, J.T.; Leong, K.W. Chitosan-DNA nanoparticles as gene carriers: synthesis, characterization and transfection efficiency. *J. Control. Release* **2001**, *70*, 399–421.
141. Corsi, K.; Chellat, F.; Yahia, L.; Fernandes, J.C. Mesenchymal stem cells, MG63 and HEK293 transfection using chitosan-DNA nanoparticles. *Biomaterials* **2003**, *24*, 1255–64.
142. Jayakumar, R.; Chennazhi, K.P.; Muzzarelli, R.A.A.; Tamura, H.; Nair, S.V.;

Selvamurugan, N. Chitosan conjugated DNA nanoparticles in gene therapy. *Carbohydr. Polym.* **2010**, *79*, 1–8.

143. MacLaughlin, F.C.; Mumper, R.J.; Wang, J.; Tagliaferri, J.M.; Gill, I.; Hinchcliffe, M.; Rolland, A.P. Chitosan and depolymerized chitosan oligomers as condensing carriers for in vivo plasmid delivery. *J. Control. Release* **1998**, *56*, 259–272.
144. Venkatesh, S.; Smith, T.J. Chitosan-membrane interactions and their probable role in chitosan-mediated transfection. *Biotechnol. Appl. Biochem.* **1998**, *27*, 265–7.
145. Zhu, H.; Cao, J.; Cui, S.; Qian, Z.; Gu, Y. Enhanced Tumor Targeting and Antitumor Efficacy via Hydroxycamptothecin-Encapsulated Folate-Modified N-Succinyl-N′-Octyl Chitosan Micelles. *J. Pharm. Sci.* **2013**, *102*, 1318–1332.
146. Gu, Y.; Li, S.; Feng, S.; Ding, L.; Liu, Y.; Zhu, Q.; Qian, Z. Nanomedicine engulfed by macrophages for targeted tumor therapy. *Int. J. Nanomedicine* **2016**, *Volume 11*, 4107–4124.
147. Zhang, C.; Ding, Y.; Yu, L. (Lucy); Ping, Q. Polymeric micelle systems of hydroxycamptothecin based on amphiphilic N-alkyl-N-trimethyl chitosan derivatives. *Colloids Surfaces B Biointerfaces* **2007**, *55*, 192–199.
148. Zhang, F.; Fei, J.; Sun, M.; Ping, Q. Heparin modification enhances the delivery and tumor targeting of paclitaxel-loaded N -octyl- N -trimethyl chitosan micelles. *Int. J. Pharm.* **2016**, *511*, 390–402.
149. Mo, R.; Jin, X.; Li, N.; Ju, C.; Sun, M.; Zhang, C.; Ping, Q. The mechanism of enhancement on oral absorption of paclitaxel by N-octyl-O-sulfate chitosan micelles. *Biomaterials* **2011**, *32*, 4609–4620.
150. Mo, R.; Xiao, Y.; Sun, M.; Zhang, C.; Ping, Q. Enhancing effect of N-octyl-O-sulfate chitosan on etoposide absorption. *Int. J. Pharm.* **2011**, *409*, 38–45.
151. Jin, X.; Mo, R.; Ding, Y.; Zheng, W.; Zhang, C. Paclitaxel-Loaded *N* -Octyl- *O* -sulfate Chitosan Micelles for Superior Cancer Therapeutic Efficacy and

Overcoming Drug Resistance. *Mol. Pharm.* **2014**, *11*, 145–157.

152. Qu, G.; Wu, X.; Yin, L.; Zhang, C. N-octyl-O-sulfate chitosan-modified liposomes for delivery of docetaxel: Preparation, characterization, and pharmacokinetics. *Biomed. Pharmacother.* **2012**, *66*, 46–51.
153. Zhong, Z.; Zhong, Z.; Xing, R.; Li, P.; Mo, G. The preparation and antioxidant activity of 2-[phenylhydrazine (or hydrazine)-thiosemicarbazone]-chitosan. *Int. J. Biol. Macromol.* **2010**, *47*, 93–97.
154. Chen, X.; Cao, X.; Jiang, H.; Che, X.; Xu, X.; Ma, B.; Zhang, J.; Huang, T. SIKVAV-Modified Chitosan Hydrogel as a Skin Substitutes for Wound Closure in Mice. *Molecules* **2018**, *23*, 2611.
155. Liu, W.; Wang, F.; Zhu, Y.; Li, X.; Liu, X.; Pang, J.; Pan, W. Galactosylated Chitosan-Functionalized Mesoporous Silica Nanoparticle Loading by Calcium Leucovorin for Colon Cancer Cell-Targeted Drug Delivery. *Molecules* **2018**, *23*.
156. Zariwala, M.G.; Bendre, H.; Markiv, A.; Farnaud, S.; Renshaw, D.; Taylor, K.M.; Somavarapu, S. Hydrophobically modified chitosan nanoliposomes for intestinal drug delivery. *Int. J. Nanomedicine* **2018**, *13*, 5837–5848.
157. Chiesa, E.; Dorati, R.; Conti, B.; Modena, T.; Cova, E.; Meloni, F.; Genta, I. Hyaluronic Acid-Decorated Chitosan Nanoparticles for CD44-Targeted Delivery of Everolimus. *Int. J. Mol. Sci.* **2018**, *19*.
158. Kim, G.H.; Won, J.E.; Byeon, Y.; Kim, M.G.; Wi, T.I.; Lee, J.M.; Park, Y.-Y.; Lee, J.-W.; Kang, T.H.; Jung, I.D.; et al. Selective delivery of PLXDC1 small interfering RNA to endothelial cells for anti-angiogenesis tumor therapy using CD44-targeted chitosan nanoparticles for epithelial ovarian cancer. *Drug Deliv.* **2018**, *25*, 1394–1402.
159. Iglesias, N.; Galbis, E.; Díaz-Blanco, M.J.; Lucas, R.; Benito, E.; de-Paz, M.-V. Nanostructured Chitosan-Based Biomaterials for Sustained and Colon-Specific Resveratrol Release. *Int. J. Mol. Sci.* **2019**, *20*.

160. Chen, J.; Yang, X.; Huang, L.; Lai, H.; Gan, C.; Luo, X. Development of dual-drug-loaded stealth nanocarriers for targeted and synergistic anti-lung cancer efficacy. *Drug Deliv.* **2018**, *25*, 1932–1942.

161. Zhao, H.; Yang, J.; Qian, Q.; Wu, M.; Li, M.; Xu, W. Mesenteric CD103+DCs Initiate Switched Coxsackievirus B3 VP1-Specific IgA Response to Intranasal Chitosan-DNA Vaccine Through Secreting BAFF/IL-6 and Promoting Th17/Tfh Differentiation. *Front. Immunol.* **2018**, *9*, 2986.

162. Siddiqui, J.A.; Partridge, N.C. Physiological bone remodeling: Systemic regulation and growth factor involvement. *Physiology* 2016, *31*, 233–245.

163. Kenkre, J.S.; Bassett, J.H.D. The bone remodelling cycle. *Ann. Clin. Biochem.* 2018, *55*, 308–327.

164. Charles, J.F.; Aliprantis, A.O. Osteoclasts: More than "bone eaters." *Trends Mol. Med.* 2014, *20*, 449–459.

165. Goldring, S.R. The osteocyte: Key player in regulating bone turnover. *RMD Open* 2015, *1*, 49.

166. Itoh, K.; Udagawa, N.; Katagiri, T.; Iemura, S.; Ueno, N.; Yasuda, H.; Higashio, K.; Quinn, J.M.W.; Gillespie, M.T.; Martin, T.J.; et al. Bone Morphogenetic Protein 2 Stimulates Osteoclast Differentiation and Survival Supported by Receptor Activator of Nuclear Factor-κB Ligand. *Endocrinology* **2001**, *142*, 3656–3662.

167. Ruppert, R.; Hoffmann, E.; Sebald, W. Human Bone Morphogenetic Protein 2 Contains a Heparin-Binding Site which Modifies Its Biological Activity. *Eur. J. Biochem.* **1996**, *237*, 295–302.

168. Kawai, M.; Bessho, K.; Kaihara, S.; Sonobe, J.; Oda, K.; Iizuka, T.; Maruyama, H. Ectopic Bone Formation by Human Bone Morphogenetic Protein-2 Gene Transfer to Skeletal Muscle Using Transcutaneous Electroporation. *Hum. Gene Ther.* **2003**, *14*, 1547–1556.

169. El-Safadi, M.; Shinwari, T.; Al-Malki, S.; Manikandan, M.; Mahmood, A.; Aldahmash, A.; Alfayez, M.; Kassem, M.; Alajez, N.M. Convergence of TGFβ and BMP signaling in regulating human bone marrow stromal cell differentiation. *Sci. Rep.* **2019**, *9*, 1–13.

170. Osyczka, A.M.; Diefenderfer, D.L.; Bhargave, G.; Leboy, P.S. Different Effects of BMP-2 on Marrow Stromal Cells from Human and Rat Bone. In Proceedings of the Cells Tissues Organs; NIH Public Access, 2004; Vol. 176, pp. 109–119.

171. García-Gareta, E.; Coathup, M.J.; Blunn, G.W. Osteoinduction of bone grafting materials for bone repair and regeneration. *Bone* 2015, *81*, 112–121.

172. Nazirkar, G.; Singh, S.; Dole, V.; Nikam, A. Effortless effort in bone regeneration: a review. *J. Int. oral Heal. JIOH* **2014**, *6*, 120–124.

173. Tang, D.; Tare, R.S.; Yang, L.Y.; Williams, D.F.; Ou, K.L.; Oreffo, R.O.C. Biofabrication of bone tissue: Approaches, challenges and translation for bone regeneration. *Biomaterials* 2016, *83*, 363–382.

174. Hixon, K.R.; Lu, T.; Sell, S.A. A comprehensive review of cryogels and their roles in tissue engineering applications. *Acta Biomater.* 2017, *62*, 29–41.

175. Goor, O.J.G.M.; Hendrikse, S.I.S.; Dankers, P.Y.W.; Meijer, E.W. From supramolecular polymers to multi-component biomaterials. *Chem. Soc. Rev.* **2017**.

176. Wright, B.; Cave, R.A.; Cook, J.P.; Khutoryanskiy, V. V; Mi, S.; Chen, B.; Leyland, M.; Connon, C.J. Enhanced viability of corneal epithelial cells for efficient transport/storage using a structurally modified calcium alginate hydrogel. *Regen. Med.* **2012**, *7*, 295–307.

177. Caló, E.; Khutoryanskiy, V. V. Biomedical applications of hydrogels: A review of patents and commercial products. *Eur. Polym. J.* 2015, *65*, 252–267.

178. Berillo, D.; Mattiasson, B.; Galaev, I.Y.; Kirsebom, H. Formation of macroporous self-assembled hydrogels through cryogelation of Fmoc-Phe-Phe. *J. Colloid*

Interface Sci. **2012**, *368*, 226–230.

179. Kirsebom, H.; Elowsson, L.; Berillo, D.; Cozzi, S.; Inci, I.; Piskin, E.; Galaev, I.Y.; Mattiasson, B. Enzyme-Catalyzed Crosslinking in a Partly Frozen State: A New Way to Produce Supermacroporous Protein Structures. *Macromol. Biosci.* **2013**, *13*, 67–76.
180. Abueva, C.D.G.; Padalhin, A.R.; Min, Y.K.; Lee, B.T. Preformed chitosan cryogel-biphasic calcium phosphate: A potential injectable biocomposite for pathologic fracture. *J. Biomater. Appl.* **2015**, *30*, 182–192.
181. Lozinsky, V.I.; Galaev, I.Y.; Plieva, F.M.; Savina, I.N.; Jungvid, H.; Mattiasson, B. Polymeric cryogels as promising materials of biotechnological interest. *Trends Biotechnol.* 2003, *21*, 445–451.
182. Florencio-Silva, R.; Sasso, G.R.D.S.; Sasso-Cerri, E.; Simões, M.J.; Cerri, P.S. Biology of Bone Tissue: Structure, Function, and Factors That Influence Bone Cells. *Biomed Res. Int.* 2015, *2015*.
183. Berendsen, A.D.; Olsen, B.R. Bone development. *Bone* 2015, *80*, 14–18.
184. Zhang, X.; Chang, W.; Lee, P.; Wang, Y.; Yang, M.; Li, J.; Kumbar, S.G.; Yu, X. Polymer-ceramic spiral structured scaffolds for bone tissue engineering: effect of hydroxyapatite composition on human fetal osteoblasts. *PLoS One* **2014**, *9*, e85871.
185. Surmenev, R.A.; Surmeneva, M.A.; Ivanova, A.A. Significance of calcium phosphate coatings for the enhancement of new bone osteogenesis--a review. *Acta Biomater.* **2014**, *10*, 557–579.
186. Bhardwaj, N.; Devi, D.; Mandal, B.B. Tissue-engineered cartilage: The crossroads of biomaterials, cells and stimulating factors. *Macromol. Biosci.* 2015, *15*, 153–182.
187. He, Q.; Ao, Q.; Gong, K.; Zhang, L.; Hu, M.; Gong, Y.; Zhang, X. Preparation and characterization of chitosan-heparin composite matrices for blood

contacting tissue engineering. *Biomed. Mater.* **2010**, *5*.

188. Madihally, S. V; Matthew, H.W. Porous chitosan scaffolds for tissue engineering. *Biomaterials* **1999**, *20*, 1133–42.
189. Cheung, H.Y.; Brown, M.R. Evaluation of glycine as an inactivator of glutaraldehyde. *J. Pharm. Pharmacol.* **1982**, *34*, 211–214.
190. Singh, N.K.; Dsouza, R.N.; Grasselli, M.; Fernández-Lahore, M. High capacity cryogel-type adsorbents for protein purification. *J. Chromatogr. A* **2014**, *1355*, 143–148.
191. Song, Y.; Mathias, P.M.; Tremblay, D.; Chen, C.-C. Liquid Viscosity Model for Polymer Solutions and Mixtures. *Ind. Eng. Chem. Res.* **2003**, *42*, 2415–2422.
192. Dmitriy, B. Gold nanoparticles incorporated into cryogel walls for efficient nitrophenol conversion. *J. Clean. Prod.* **2020**, *247*, 119089.
193. Grant, D.; Long, W.F.; Moffat, C.F.; Williamson, F.B. Infrared spectroscopy of heparins suggests that the region 750-950 cm- ’ is sensitive to changes in iduronate residue ring conformation. **2000**, *275*, 193–197.
194. Gun’ko, V.M.; Savina, I.N.; Mikhalovsky, S. V. Cryogels: Morphological, structural and adsorption characterisation. *Adv. Colloid Interface Sci.* **2013**, *187–188*, 1–46.
195. Lozinsky, V.I. A brief history of polymeric cryogels. *Adv. Polym. Sci.* **2014**, *263*.
196. Jain, E.; Kumar, A. Disposable polymeric cryogel bioreactor matrix for therapeutic protein production. *Nat. Protoc.* **2013**, *8*, 821–835.
197. Zaushitsyna, O.; Berillo, D.; Kirsebom, H.; Mattiasson, B. Cryostructured and crosslinked viable cells forming monoliths suitable for bioreactor applications. *Top. Catal.* **2014**, *57*, 339–348.
198. Ingavle, G.C.; Baillie, L.W.J.; Zheng, Y.; Lis, E.K.; Savina, I.N.; Howell, C.A.; Mikhalovsky, S. V.; Sandeman, S.R. Affinity binding of antibodies to supermacroporous cryogel adsorbents with immobilized protein A for removal

of anthrax toxin protective antigen. *Biomaterials* **2015**, *50*, 140–153.

199. Katsen-Globa, A.; Meiser, I.; Petrenko, Y.A.; Ivanov, R. V.; Lozinsky, V.I.; Zimmermann, H.; Petrenko, A.Y. Towards ready-to-use 3-D scaffolds for regenerative medicine: Adhesion-based cryopreservation of human mesenchymal stem cells attached and spread within alginate-gelatin cryogel scaffolds. *J. Mater. Sci. Mater. Med.* **2014**, *25*, 857–871.
200. Plieva, F.M.; Galaev, I.Y.; Noppe, W.; Mattiasson, B. Cryogel applications in microbiology. *Trends Microbiol.* **2008**, *16*, 543–551.
201. Kumar, A.; Srivastava, A. Cell separation using cryogel-based affinity chromatography. *Nat. Protoc.* **2010**, *5*, 1737–1747.
202. Dainiak, M.B.; Allan, I.U.; Savina, I.N.; Cornelio, L.; James, E.S.; James, S.L.; Mikhalovsky, S. V; Jungvid, H.; Galaev, I.Y. Gelatin-fibrinogen cryogel dermal matrices for wound repair: preparation, optimisation and in vitro study. *Biomaterials* **2010**, *31*, 67–76.
203. Gandhi, N.S.; Mancera, R.L. Prediction of heparin binding sites in bone morphogenetic proteins (BMPs). *Biochim. Biophys. Acta - Proteins Proteomics* **2012**, *1824*, 1374–1381.
204. Smith, R.A.A.; Murali, S.; Rai, B.; Lu, X.; Lim, Z.X.H.; Lee, J.J.L.; Nurcombe, V.; Cool, S.M. Minimum structural requirements for BMP-2-binding of heparin oligosaccharides. *Biomaterials* **2018**, *184*, 41–55.
205. Dong, X.; Wang, Q.; Wu, T.; Pan, H. Understanding adsorption-desorption dynamics of BMP-2 on hydroxyapatite (001) surface. *Biophys. J.* **2007**, *93*, 750–9.
206. Shalumon, K.T.; Kuo, C.-Y.; Wong, C.-B.; Chien, Y.-M.; Chen, H.-A.; Chen, J.-P. Gelatin/Nanohyroxyapatite Cryogel Embedded Poly(lactic-co-glycolic Acid)/Nanohydroxyapatite Microsphere Hybrid Scaffolds for Simultaneous Bone Regeneration and Load-Bearing. *Polymers (Basel).* **2018**, *10*.
207. Kwon, S.; Lee, S.S.; Sivashanmugam, A.; Kwon, J.; Kim, S.H.L.; Noh, M.Y.;

Kwon, S.K.; Jayakumar, R.; Hwang, N.S. Bioglass-Incorporated Methacrylated Gelatin Cryogel for Regeneration of Bone Defects. *Polymers (Basel).* **2018**, *10*.

208. Gu, L.; Zhang, J.; Li, L.; Du, Z.; Cai, Q.; Yang, X. Hydroxyapatite nanowire composited gelatin cryogel with improved mechanical properties and cell migration for bone regeneration. *Biomed. Mater.* **2019**, *14*, 045001.
209. Hixon, K.R.; Melvin, A.M.; Lin, A.Y.; Hall, A.F.; Sell, S.A. Cryogel scaffolds from patient-specific 3D-printed molds for personalized tissue-engineered bone regeneration in pediatric cleft-craniofacial defects. *J. Biomater. Appl.* **2017**, *32*, 598–611.
210. Hixon, K.R.; Eberlin, C.T.; Lu, T.; Neal, S.M.; Case, N.D.; McBride-Gagyi, S.H.; Sell, S.A. The calcification potential of cryogel scaffolds incorporated with various forms of hydroxyapatite for bone regeneration. *Biomed. Mater.* **2017**, *12*, 025005.
211. Raina, D.B.; Isaksson, H.; Teotia, A.K.; Lidgren, L.; Tägil, M.; Kumar, A. Biocomposite macroporous cryogels as potential carrier scaffolds for bone active agents augmenting bone regeneration. *J. Control. Release* **2016**, *235*, 365–378.
212. Salgado, C.L.; Grenho, L.; Fernandes, M.H.; Colaço, B.J.; Monteiro, F.J. Biodegradation, biocompatibility, and osteoconduction evaluation of collagen-nanohydroxyapatite cryogels for bone tissue regeneration. *J. Biomed. Mater. Res. Part A* **2016**, *104*, 57–70.
213. Jayasuriya, A.C.; Mauch, K.J. In vitro degradation behavior of chitosan based hybrid microparticles. *J. Biomed. Sci. Eng.* **2011**, *4*, 383–390.
214. Foster, L.J.R.; Ho, S.; Hook, J.; Basuki, M.; Marçal, H. Chitosan as a Biomaterial: Influence of Degree of Deacetylation on Its Physiochemical, Material and Biological Properties. *PLoS One* **2015**, *10*, e0135153.
215. Freier, T.; Koh, H.S.; Kazazian, K.; Shoichet, M.S. Controlling cell adhesion and

degradation of chitosan films by N-acetylation. *Biomaterials* **2005**, *26*, 5872–5878.

216. Neamtu, I.; Chiriac, A.P.; Nita, L.E.; Bercea, M. Poly(aspartic acid) in interpolymer complex with biomedical applications. *J. Optoelectron. Adv. Mater.* **2007**, *9*, 3459–3462.
217. Kantoğlu, Ö.; Çaykara, T.; Güven, O. Preparation and characterization of polysaccaride interpolymer complexes: I-PVA/ι-carrageenan. *J. Appl. Polym. Sci.* **2013**, *127*, 500–507.
218. Bizley, S.C.; Williams, A.C.; Khutoryanskiy, V. V Thermodynamic and kinetic properties of interpolymer complexes assessed by isothermal titration calorimetry and surface plasmon resonance. *Soft Matter* **2014**, *10*, 8254–8260.
219. Rodrigues, M.; Kosaric, N.; Bonham, C.A.; Gurtner, G.C. Wound healing: A cellular perspective. *Physiol. Rev.* **2019**, *99*, 665–706.
220. Saparov, A.; Ogay, V.; Nurgozhin, T.; Chen, W.C.W.; Mansurov, N.; Issabekova, A.; Zhakupova, J. Role of the immune system in cardiac tissue damage and repair following myocardial infarction. *Inflamm. Res.* 2017, *66*, 739–751.
221. Brazil, J.C.; Quiros, M.; Nusrat, A.; Parkos, C.A. Innate immune cell–epithelial crosstalk during wound repair. *J. Clin. Invest.* 2019, *129*, 2983–2993.
222. Jorch, S.K.; Kubes, P. An emerging role for neutrophil extracellular traps in noninfectious disease. *Nat. Med.* 2017, *23*, 279–287.
223. Castaño, O.; Pérez-Amodio, S.; Navarro-Requena, C.; Mateos-Timoneda, M.Á.; Engel, E. Instructive microenvironments in skin wound healing: Biomaterials as signal releasing platforms. *Adv. Drug Deliv. Rev.* 2018, *129*, 95–117.
224. Martin, P.; Nunan, R. Cellular and molecular mechanisms of repair in acute and chronic wound healing. *Br. J. Dermatol.* 2015, *173*, 370–378.
225. Sun, B.K.; Siprashvili, Z.; Khavari, P.A. Advances in skin grafting and treatment of cutaneous wounds. *Science (80-.).* 2014, *346*, 941–945.
226. Cordeiro, J. V; Jacinto, A. The role of transcription-independent damage signals

in the initiation of epithelial Cordeiro, J. V, & Jacinto, A. (2013). The role of transcription-independent damage signals in the initiation of epithelial wound healing. Nature reviews. Molecular cell b. *Nat. Rev. Mol. Cell Biol.* **2013**, *14*, 249–62.

227. Goh, M.C.; Hwang, Y.; Tae, G. Epidermal growth factor loaded heparin-based hydrogel sheet for skin wound healing. *Carbohydr. Polym.* **2016**, *147*, 251–260.
228. Liu, J.M.H.; Zhang, J.; Zhang, X.; Hlavaty, K.A.; Ricci, C.F.; Leonard, J.N.; Shea, L.D.; Gower, R.M. Transforming growth factor-beta 1 delivery from microporous scaffolds decreases inflammation post-implant and enhances function of transplanted islets. *Biomaterials* **2016**, *80*, 11–19.
229. Riabov, V.; Salazar, F.; Htwe, S.S.; Gudima, A.; Schmuttermaier, C.; Barthes, J.; Knopf-Marques, H.; Klüter, H.; Ghaemmaghami, A.M.; Vrana, N.E.; et al. Generation of anti-inflammatory macrophages for implants and regenerative medicine using self-standing release systems with a phenotype-fixing cytokine cocktail formulation. *Acta Biomater.* **2017**, *53*, 389–398.
230. Losi, P.; Briganti, E.; Errico, C.; Lisella, A.; Sanguinetti, E.; Chiellini, F.; Soldani, G. Fibrin-based scaffold incorporating VEGF- and bFGF-loaded nanoparticles stimulates wound healing in diabetic mice. *Acta Biomater.* **2013**, *9*, 7814–21.
231. Wang, H.M.; Chou, Y.T.; Wen, Z.H.; Wang, Z.R.; Chen, C.H.; Ho, M.L. Novel Biodegradable Porous Scaffold Applied to Skin Regeneration. *PLoS One* **2013**, *8*, 2–12.
232. Xie, L.; Law, B.K.; Aakre, M.E.; Edgerton, M.; Shyr, Y.; Bhowmick, N.A.; Moses, H.L. Transforming growth factor beta-regulated gene expression in a mouse mammary gland epithelial cell line. *Breast Cancer Res.* **2003**, *5*.
233. Thompson-Snipes, L.; Dhar, V.; Bond, M.W.; Mosmann, T.R.; Moore, K.W.; Rennick, D.M. Interleukin 10: A novel stimulatory factor for mast cells and their progenitors. *J. Exp. Med.* **1991**, *173*, 507–510.

234. Marinval, N.; Morenc, M.; Labour, M.N.; Samotus, A.; Mzyk, A.; Ollivier, V.; Maire, M.; Jesse, K.; Bassand, K.; Niemiec-Cyganek, A.; et al. Fucoidan/VEGF-based surface modification of decellularized pulmonary heart valve improves the antithrombotic and re-endothelialization potential of bioprostheses. *Biomaterials* **2018**, *172*, 14–29.

235. Igarashi, M.; Finch, P.W.; Aaronson, S.A. Characterization of recombinant human fibroblast growth factor (FGF)-10 reveals functional similarities with keratinocyte growth factor (FGF-7). *J. Biol. Chem.* **1998**, *273*, 13230–13235.

236. Jimi, S.; De Francesco, F.; Ferraro, G.A.; Riccio, M.; Hara, S. A Novel Skin Splint for Accurately Mapping Dermal Remodeling and Epithelialization During Wound Healing. *J. Cell. Physiol.* **2017**, *232*, 1225–1232.

237. Reinke, J.M.; Sorg, H. Wound repair and regeneration. *Eur. Surg. Res.* 2012, *49*, 35–43.

238. Chung, L.; Maestas, D.R.; Housseau, F.; Elisseeff, J.H. Key players in the immune response to biomaterial scaffolds for regenerative medicine. *Adv. Drug Deliv. Rev.* 2017, *114*, 184–192.

239. Mittal, M.; Siddiqui, M.R.; Tran, K.; Reddy, S.P.; Malik, A.B. Reactive oxygen species in inflammation and tissue injury. *Antioxidants Redox Signal.* 2014, *20*, 1126–1167.

240. Dahlgren, M.W.; Molofsky, A.B. Adventitial Cuffs: Regional Hubs for Tissue Immunity. *Trends Immunol.* 2019, *40*, 877–887.

241. Chou, C.; Li, M.O. Tissue-resident lymphocytes across innate and adaptive lineages. *Front. Immunol.* 2018, *9*.

242. Chen, H.; Cheng, J.; Ran, L.; Yu, K.; Lu, B.; Lan, G.; Dai, F.; Lu, F. An injectable self-healing hydrogel with adhesive and antibacterial properties effectively promotes wound healing. *Carbohydr. Polym.* **2018**, *201*, 522–531.

243. Zhao, X.; Wu, H.; Guo, B.; Dong, R.; Qiu, Y.; Ma, P.X. Antibacterial anti-oxidant

electroactive injectable hydrogel as self-healing wound dressing with hemostasis and adhesiveness for cutaneous wound healing. *Biomaterials* **2017**, *122*, 34–47.

244. Re-epithelialization of adult skin wounds: Cellular mechanisms and therapeutic strategies. - PubMed - NCBI Available online: https://www.ncbi.nlm.nih.gov/pubmed/29981800 (accessed on May 2, 2020).

245. You, C.; Li, Q.; Wang, X.; Wu, P.; Ho, J.K.; Jin, R.; Zhang, L.; Shao, H.; Han, C. Silver nanoparticle loaded collagen/chitosan scaffolds promote wound healing via regulating fibroblast migration and macrophage activation. *Sci. Rep.* **2017**, *7*, 10489.

246. Hamedi, H.; Moradi, S.; Hudson, S.M.; Tonelli, A.E. Chitosan based hydrogels and their applications for drug delivery in wound dressings: A review. *Carbohydr. Polym.* 2018, *199*, 445–460.